

DEVELOPMENT OF ADVANCED NO<sub>x</sub> CONTROL CONCEPTS  
FOR COAL-FIRED UTILITY BOILERS

DOE Contract No. DE-AC22-90PC90363

Period of Performance: September 26, 1990 to October 26, 1992

DOE/PC/90363--T8

DE93 012455

**Quarterly Technical Progress Report No. 8**

Period Covered by Report: July 1, 1992 to September 30, 1992

prepared by:

A. Evans  
J. Newhall Pont  
G. England  
W.R. Seeker

Energy and Environmental Research Corporation  
18 Mason  
Irvine, California 92718

Date Submitted: March 4, 1993

prepared for:

Mr. Charles E. Schmidt  
U. S. Department of Energy  
Pittsburgh Energy Technology Center  
P. O. Box 10940  
Pittsburgh, Pennsylvania 15236-0940

**MASTER**

DISTRIBUTION OF THIS DOCUMENT IS UNLIMITED

*js*

*BD*

## TABLE OF CONTENTS

<u>Section</u>	<u>Page</u>
1.0 INTRODUCTION .....	1-1
2.0 ADVANCED REBURNING RESULTS .....	2-1
2.1 EFFECT OF UREA INJECTION TEMPERATURE .....	2-1
2.2 EFFECT OF REBURN ZONE STOICHIOMETRY .....	2-3
2.3 EFFECT OF BURNOUT AIR INJECTION LOCATION .....	2-11
2.4 EFFECT OF INJECTED UREA CONCENTRATION .....	2-18
3.0 METHANOL INJECTION RESULTS .....	3-1
4.0 PILOT-SCALE SCRUBBING STUDIES RESULTS .....	4-1
5.0 SUMMARY .....	5-1

### DISCLAIMER

This report was prepared as an account of work sponsored by an agency of the United States Government. Neither the United States Government nor any agency thereof, nor any of their employees, makes any warranty, express or implied, or assumes any legal liability or responsibility for the accuracy, completeness, or usefulness of any information, apparatus, product, or process disclosed, or represents that its use would not infringe privately owned rights. Reference herein to any specific commercial product, process, or service by trade name, trademark, manufacturer, or otherwise does not necessarily constitute or imply its endorsement, recommendation, or favoring by the United States Government or any agency thereof. The views and opinions of authors expressed herein do not necessarily state or reflect those of the United States Government or any agency thereof.

## LIST OF FIGURES

<u>Figure</u>	<u>Page</u>
1-1 Application of CombiNO <sub>x</sub> to a coal-fired utility boiler .....	1-2
1-2 EER's 10 Million Btu/hr Reburn Tower .....	1-4
2-1 Effect of urea injection temperature on Advanced Reburning performance and by-product formation .....	2-2
2-2 Effect of reburn zone stoichiometry on Advanced Reburning performance .....	2-4
2-3 Effect of reburn stoichiometry on urea performance at the CTT and BSF .....	2-6
2-4 Effect of SR <sub>2</sub> and temperature on urea performance .....	2-7
2-5 Effect of final oxygen content on urea performance .....	2-8
2-6 Effect of burnout air addition on urea performance at the BSF .....	2-9
2-7 Effect of reburn zone stoichiometry on Advanced Reburning performance .....	2-10
2-8 Temperature window breadth below NO <sub>f</sub> /NO <sub>i</sub> = 60% as a function of SR <sub>2</sub> .....	2-12
2-9 Effect of reburn zone stoichiometry on N <sub>2</sub> O emissions .....	2-13
2-10 N <sub>2</sub> O formation as a function of SR <sub>2</sub> and urea injection temperature .....	2-14
2-11 N <sub>2</sub> O formation as a result of NO reduction .....	2-15
2-12 N <sub>2</sub> O formation as a function of reburn zone stoichiometry and NO reduction .....	2-16
2-13 Effect of burnout air injection location on urea performance .....	2-17
2-14 Effect of urea concentration on Advanced Reburning performance and N <sub>2</sub> O formation .....	2-20
2-15 Overall CombiNO <sub>x</sub> performance at the Reburn Tower .....	2-21
3-1 Effect of methanol concentration on performance and by-product formation .....	3-2
3-2 Reburn Tower sample ports for NO <sub>2</sub> to NO re-conversion .....	3-4
3-3 Reburn Tower NO <sub>2</sub> to NO re-conversion .....	3-6
3-4 NASA equilibrium model results .....	3-7

3-5	Effect of residence time o NO <sub>2</sub> to NO re-conversion .....	3-8
3-6	Quench rate comparison between Reburn Tower and full-scale, Hennepin Station ..	3-9
4-1	Research Cottrell's pilot-scale scrubbing apparatus .....	4-2
4-2	Effect of liquid to gas ratio on NO <sub>2</sub> scrubbing efficiency .....	4-4
4-3	Effect of initial NO <sub>2</sub> concentration on NO <sub>2</sub> removal efficiency .....	4-5
4-4	Effect of Na <sub>2</sub> CO <sub>3</sub> dilution on NO <sub>2</sub> scrubbing performance .....	4-6
5-1	NO <sub>x</sub> reduction for the integrated CombiNO <sub>x</sub> process .....	5-2

## 1.0 INTRODUCTION

Hybrid technologies for the reduction of NO<sub>x</sub> emissions from coal-fired utility boilers have shown the potential to offer greater levels of NO<sub>x</sub> control than the sum of the individual technologies, leading to more cost effective emissions control strategies. Energy and Environmental Research Corporation (EER) has developed a hybrid NO<sub>x</sub> control strategy involving two proprietary concepts which has the potential to meet the U.S. Department of Energy's NO<sub>x</sub> reduction goal at a significant reduction in cost compared to existing technology. The process has been named CombiNO<sub>x</sub>.

CombiNO<sub>x</sub> is an integration of three technologies: modified reburning, promoted selective non-catalytic reduction (SNCR) and methanol injection. These technologies are combined to achieve high levels of NO<sub>x</sub> emission reduction from coal-fired power plants equipped with SO<sub>2</sub> scrubbers. The first two steps, modified reburning and promoted SNCR are linked. It has been shown that performance of the SNCR agent is dependent upon local oxidation of CO. Reburning is used to generate the optimum amount of CO to promote the SNCR agent. Approximately 10 percent reburning is required, this represents half of that required for conventional reburning. If the reburn fuel is natural gas, the combination of reburning and SNCR may result in a significant cost savings over conventional reburning. The third step, injection of methanol into the flue gas, is used to oxidize NO to NO<sub>2</sub> which may subsequently be removed in a wet scrubber. Figure 1-1 illustrates how CombiNO<sub>x</sub> may be applied to a coal-fired utility boiler.

The experimental program was divided into two phases, Fundamental Studies and Process Studies. The primary goal of the Fundamental Studies phase was to analyze the individual steps of the CombiNO<sub>x</sub> process at laboratory and pilot-scale levels. The potential synergism between the individual processes was also evaluated. During these pilot-scale tests, CombiNO<sub>x</sub> demonstrated 92 percent NO<sub>x</sub> reduction at EER's Boiler Simulation Furnace (BSF). This furnace is a 1 million Btu/hr down-fired furnace located at EER's Santa Ana Test Site. While experiments at this scale provide valuable insights into the controlling parameters of the CombiNO<sub>x</sub> process, there remain questions about whether the absolute levels of NO<sub>x</sub> reductions achieved are truly representative of what could be achieved on a utility boiler. For example, the success of the process depends to a large extent on being able to rapidly mix the reburning fuel, urea, burnout air and methanol with the flue gas. Clearly, it is much easier to accomplish good mixing in a small furnace than in a large

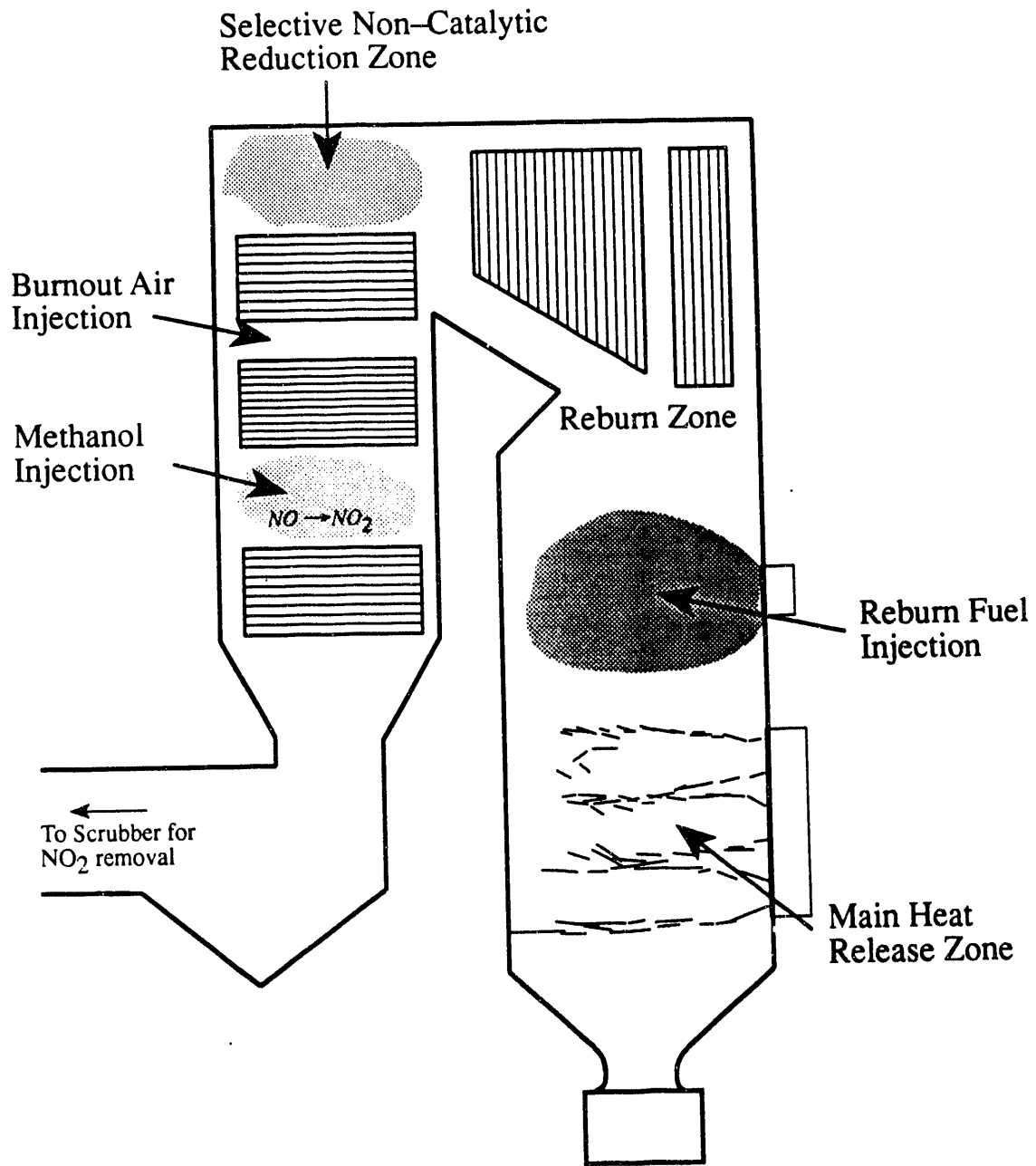


Figure 1-1. Application of CombiNO<sub>x</sub> to a coal-fired utility boiler.

utility boiler. Additionally, smaller facilities will tend to produce smaller scale mixing patterns, in particular, smaller pockets of CO and O<sub>2</sub>. Since the synergism between reburning and agent injection is related to CO/O<sub>2</sub> interactions, the smaller facilities do not necessarily yield NO<sub>x</sub> reductions representative of utility boilers. For these reasons, it is also necessary to evaluate the process at a scale that is more representative of full-scale.

The Process Studies phase of the CombiNO<sub>x</sub> program was intended to address scale-up issues of the CombiNO<sub>x</sub> process by evaluating the process on a 10 million Btu/hr furnace. The Reburn Tower, displayed in Figure 1-2, is a down-fired furnace located at EER's Santa Ana test site. It is approximately an order of magnitude larger than the small pilot-scale facility, with turbulent mixing characteristics thought to be more representative of full-scale boilers. The radiant furnace consists of 6 levels, each of which contain 14 ports for injection and sampling purposes.

Since the Reburn Tower tests are intended to reflect full-scale performance, the injection systems were designed in a manner similar to full-scale application design. This process design is discussed in detail in Quarterly Report #7.

The test results from the Reburn Tower test series are presented in this quarterly report. The primary objective of the series was to evaluate the CombiNO<sub>x</sub> process under turbulent mixing conditions. The effects of urea injection temperature, reburn zone stoichiometry, burnout air injection location, and injected urea concentration on Advanced Gas Reburning performance were evaluated. Methanol injection and NO<sub>2</sub> scrubbing tests were also conducted during the Reburn Tower tests.

Also presented in this report are the pilot-scale scrubbing studies performed by Research Cottrell. The effects of slurry flow rate, flue gas flow rate, initial NO<sub>2</sub> concentration, and slurry composition on NO<sub>2</sub> removal were observed in a liquor-modified wet limestone scrubber.

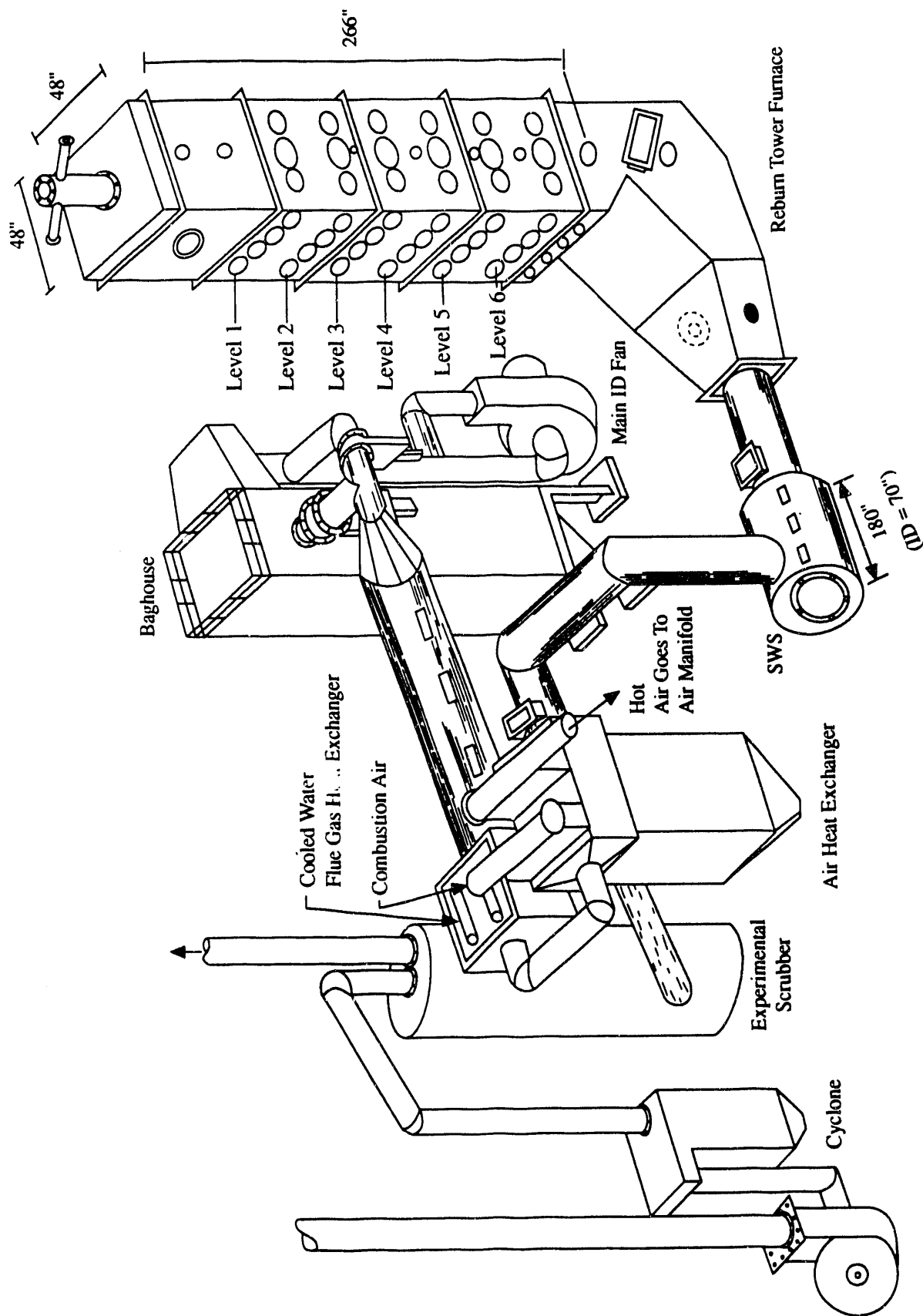


Figure 1-2. EER's 10 million Btu/hr Reburn Tower.



## 2.0 ADVANCED REBURNING RESULTS

There are several key Advanced Reburning results obtained during the Fundamental Studies phase of this program. These results include:

- There is an optimum reburn zone stoichiometry (referred to as  $SR_2$ ) in terms of SNCR enhancement. The temperature window can be broadened and deepened under the right stoichiometric conditions.
- $NO_x$  reduction performance improves as the burnout air injection is moved downstream of the reburn zone (as the reburn zone lengthens).

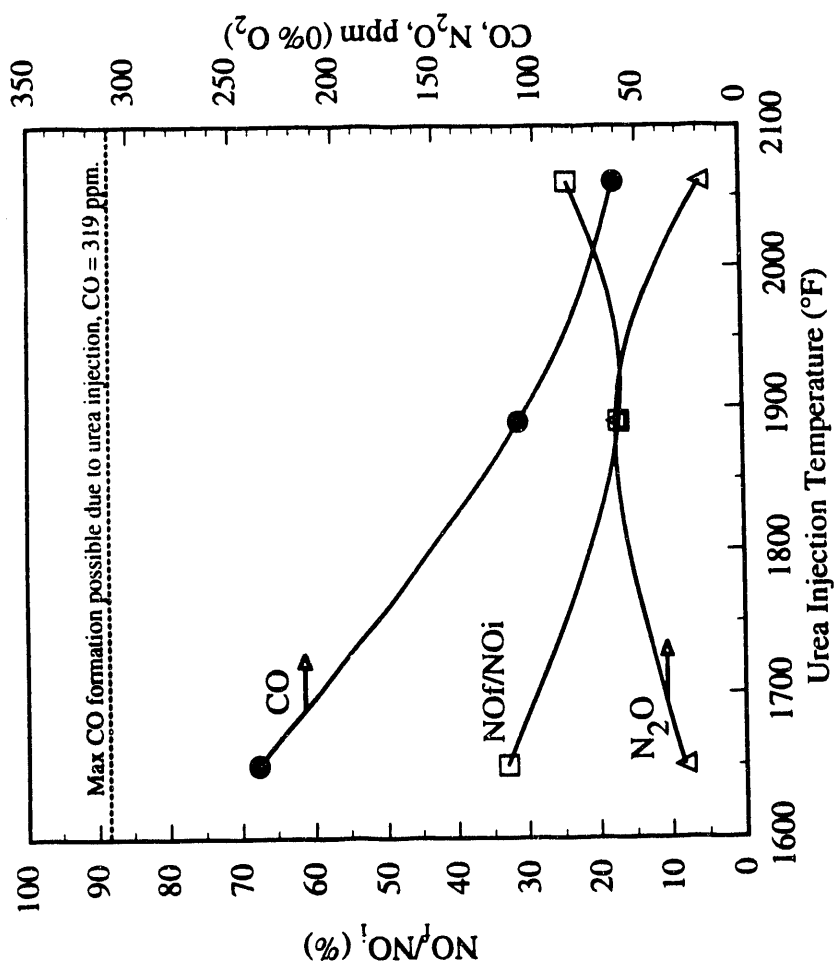
From previous tests performed on EER's smaller (0.1 MMBtu/hr) pilot-scale facility, the Controlled Temperature Tower (CTT), the following was learned:

- $NO_x$  reduction is highly sensitive to final stoichiometry. Performance is best for lower final stoichiometries.

The intent of the large pilot-scale Advanced Reburning tests was to determine if large scale turbulent mixing patterns (those more representative of full-scale) impact the process as defined in the previous studies. In other words, are the trends seen in the smaller furnaces also present at large pilot-scale. To determine this, a parametric test matrix was designed and implemented to look at the effects of reburn zone stoichiometry, urea injection temperature and burnout air injection location. The following sections present the (large pilot-scale) data, and compare them to the corresponding BSF (pilot-scale) and CTT (bench-scale) data.

### 2.1 Effect of Urea Injection Temperature

Urea was injected by means of 10 pressure atomizers positioned on 4 water-cooled lances that spanned the width of the furnace. To vary injection temperature, the lances were moved between levels 4 and 6 (see Figure 1-2). Figure 2-1 displays the effect of urea injection temperature on Advanced Reburning performance,  $N_2O$  formation, and CO emissions at the Tower Furnace. Optimum  $NO_x$  reduction occurs at approximately 1850-1900 °F, agreeing with the BSF results.

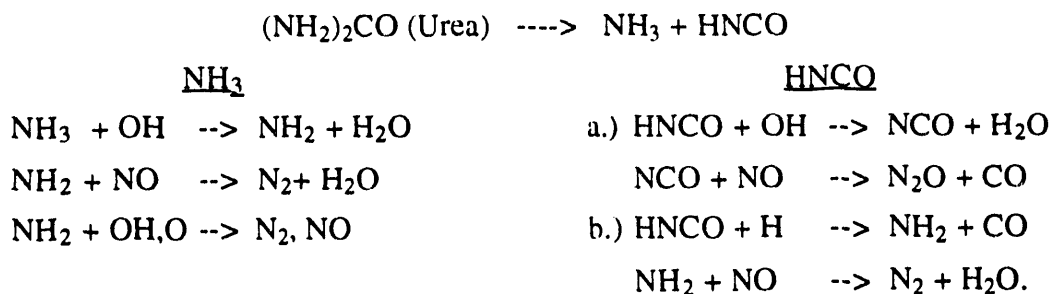


Coal Primary, NG RB  
 SR<sub>1</sub> = 1.13; SR<sub>2</sub> = 1.03; SR<sub>1</sub> = 1.20  
 Burnout air injected at same level as urea.  
 NSR = 1.5  
 NOi = approx 990 ppm  
 NOii = approx 380 ppm

Figure 2-1. Effect of urea injection temperature on Advanced Gas Reburning performance and by-product formation.

Overall Advanced Reburning performance resulted in NO<sub>x</sub> reductions of 83 percent, 89 percent reduction was achieved at the BSF.

N<sub>2</sub>O formation peaks when NO<sub>x</sub> reduction is best. This is thought to be because urea decomposes into NH<sub>3</sub> and HNCO which react in the following manner (Chen, S.L., et al. 1988).



HNCO has two possible pathways. It can be oxidized to NCO which can combine with NO to form N<sub>2</sub>O, or it can form NH<sub>2</sub> which may proceed through the de-NO<sub>x</sub> reactions. It is believed that the HNCO pathway is dependent upon stoichiometry; in a highly oxidizing environment, HNCO may be more inclined to oxidize to NCO and subsequently form N<sub>2</sub>O. At the optimum injection temperature for NO<sub>x</sub> reduction, 28 percent of the NO removed was converted to N<sub>2</sub>O. N<sub>2</sub>O formation due to urea injection is discussed in more detail in section 2.2.

CO is also a by-product of urea formation, however if the urea is injected at sufficiently high temperatures, CO can effectively oxidize to CO<sub>2</sub>. Figure 2-1 shows CO emissions to be highest when urea is injected at cooler temperatures, where oxidation of CO is less likely to occur. Maximum CO formation possible under these conditions is 319 ppm.

## 2.2 Effect of Reburn Zone and Burnout Air Injection Zone Stoichiometries

Data are now available to evaluate the effect of stoichiometry at 3 scales. Figure 2-2 shows the effect of SR<sub>2</sub> on NO reduction as a function of urea injection temperature at the BSF. The data indicate that there is an optimum level of oxidizing CO local to the urea injection point which enhances urea performance. Optimum conditions occurred at a stoichiometry of 1.02 where CO was approximately 3800 ppm and O<sub>2</sub> was 0.4 percent (dry). Similar experiments were conducted on the smaller scale CTT, indicating that optimum reburn zone stoichiometry is 0.99. Results from

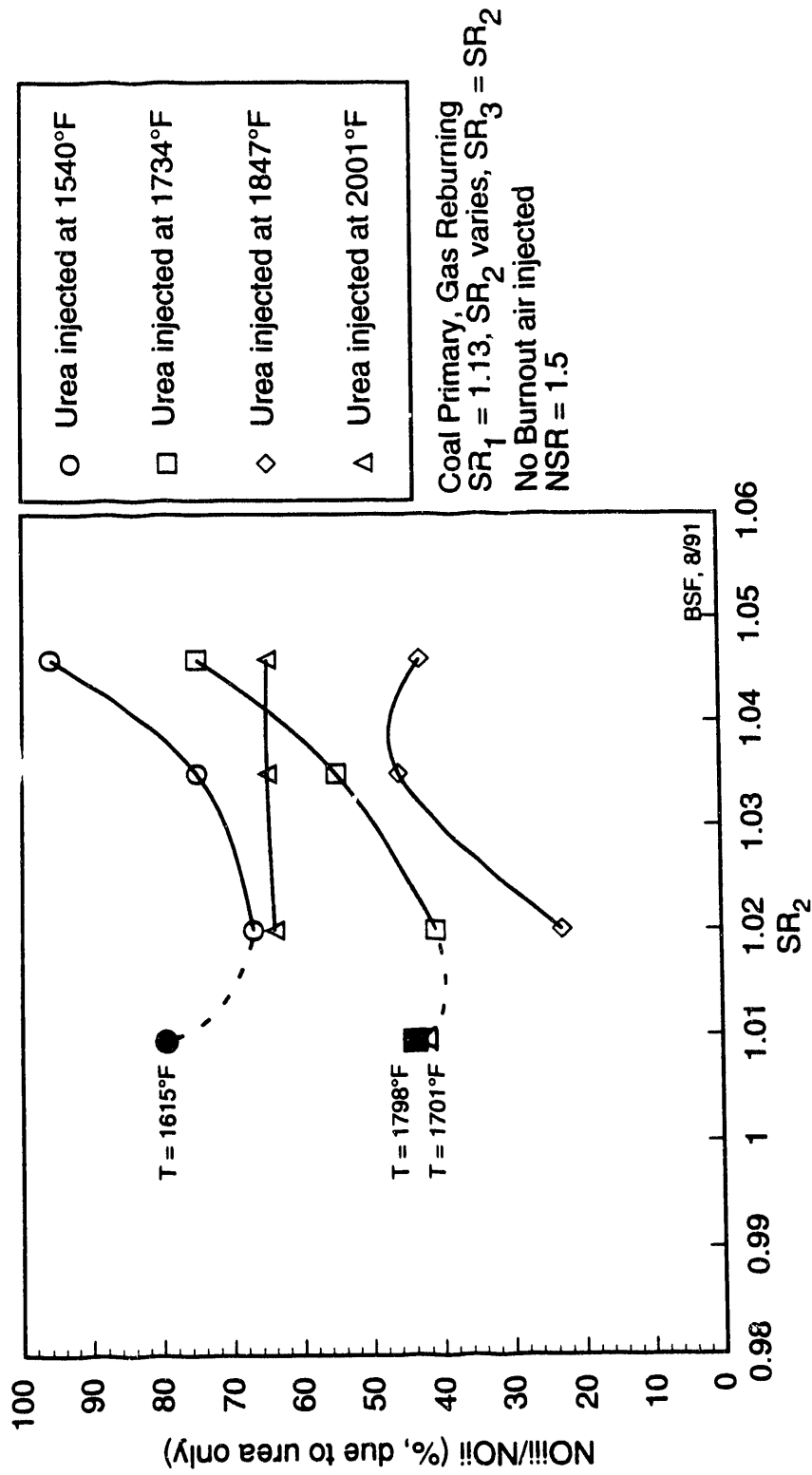


Figure 2-2. Effect of reburn zone stoichiometry on urea performance at BSF.

the CTT are compared to those of the BSF and Kinetic modeling in Figure 2-3. Similar trends were achieved in all three cases, with the BSF curve shifted slightly towards higher stoichiometries. This shift is attributed to mixing differences between the furnaces. Since the BSF is an order of magnitude larger than the CTT, the mixing of CO and O<sub>2</sub> is not as uniform. The result is a higher stoichiometry at the BSF for CO levels similar to the CTT. Since the model assumes perfect mixing, optimum conditions predicted are similar to those actually obtained at the uniformly mixed CTT.

Reburn zone stoichiometry was again varied during the Reburn Tower tests to determine how CO concentration affects performance at a larger scale. Results are displayed in Figure 2-4 as SR<sub>2</sub> was varied between 0.99 and 1.05. Contrary to the BSF results, no distinct trend was detected as SR<sub>2</sub> was varied. It has been hypothesized that the results differ between the Tower and the BSF/CTT because of the different final stoichiometries achieved. The CTT and BSF tests were performed with final stoichiometries of 1.02 - 1.05, while the Reburn Tower tests were performed with a final stoichiometry of 1.20. Figure 2-5 shows how final stoichiometry, or oxygen level, can influence urea performance. Displayed are results from all three pilot-scale furnaces, and all agree that as the final stoichiometry is increased, urea performance suffers. It can be concluded from this figure that an overabundance of radicals is detrimental to urea's performance, even when injected downstream of the urea injection point (CTT data). Performance decreases by 37% when the final oxygen content is increased from 0.4 to 3.8 percent. The fact that final oxygen content was comparatively high for all Reburn Tower tests (3.6%, dry), possibly explains why performance is poor in Figure 2-4. Performance at the Reburn Tower probably suffered severely as a result of burnout air addition, thereby "washing out" the effects of reburn zone stoichiometry. Since burnout air was not added during the BSF and CTT experiments, the influence of SR<sub>2</sub> can still be easily detected. Figure 2-6 shows the effect of burnout air addition on performance at the BSF. As the final stoichiometry is increased from 1.02 to 1.20, performance decreases by 21 percent. As suspected, performance was hampered severely when burnout air was injected, reducing the noticeable affects of SR<sub>2</sub>.

Figure 2-7 displays the same data as Figure 2-4 but with the x-axis displaying urea injection temperature. Again, it can be concluded that little difference is detected as SR<sub>2</sub> is varied and SR<sub>f</sub> remains constant at 1.20. Compared on this figure is also the scenario when urea is injected into an oxygen rich environment with a stoichiometry of 1.20 (referred to as conventional SNCR). At

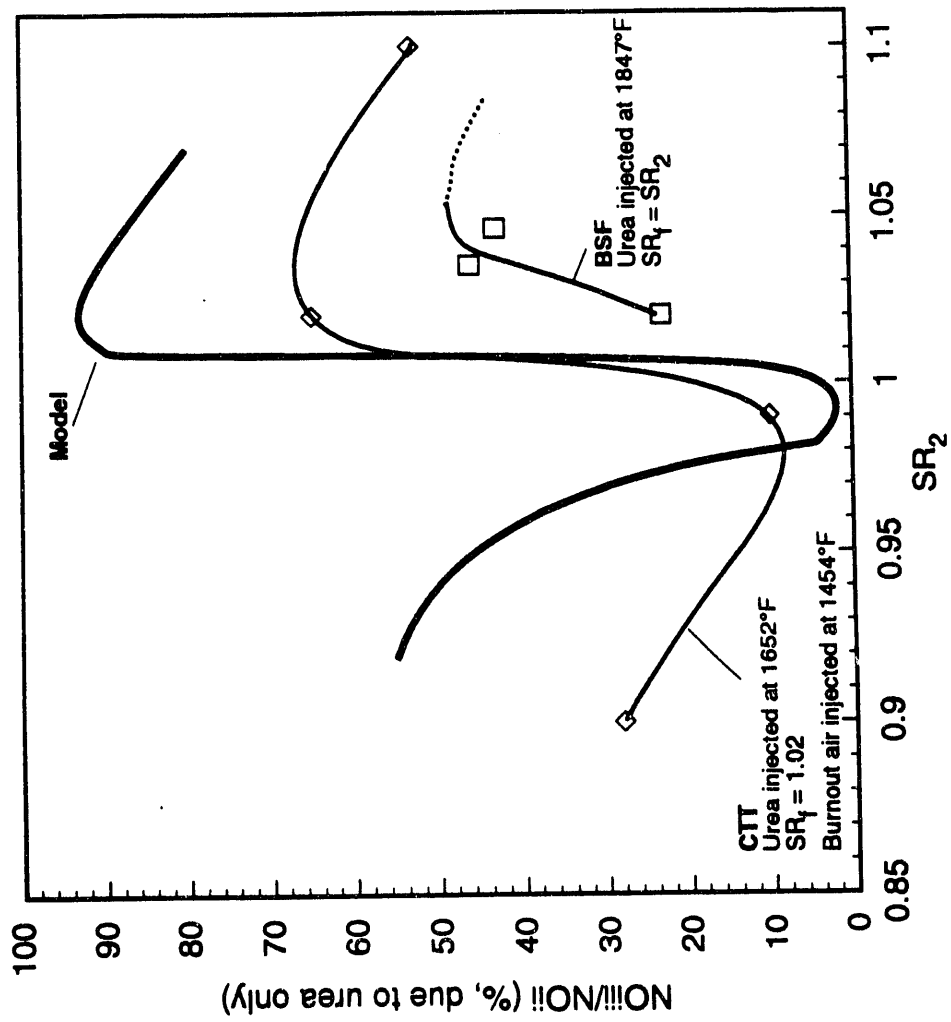


Figure 2-3. Effect of reburn zone stoichiometry on urea performance at the CTT and BSF.

Coal Primary, NG RB  
 SR<sub>1</sub> = 1.13; SR<sub>2</sub> varies; SR<sub>t</sub> = 1.2  
 Burnout air injected at same level as urea.  
 NSR = 1.5  
 NO<sub>i</sub> = approx. 990 ppm

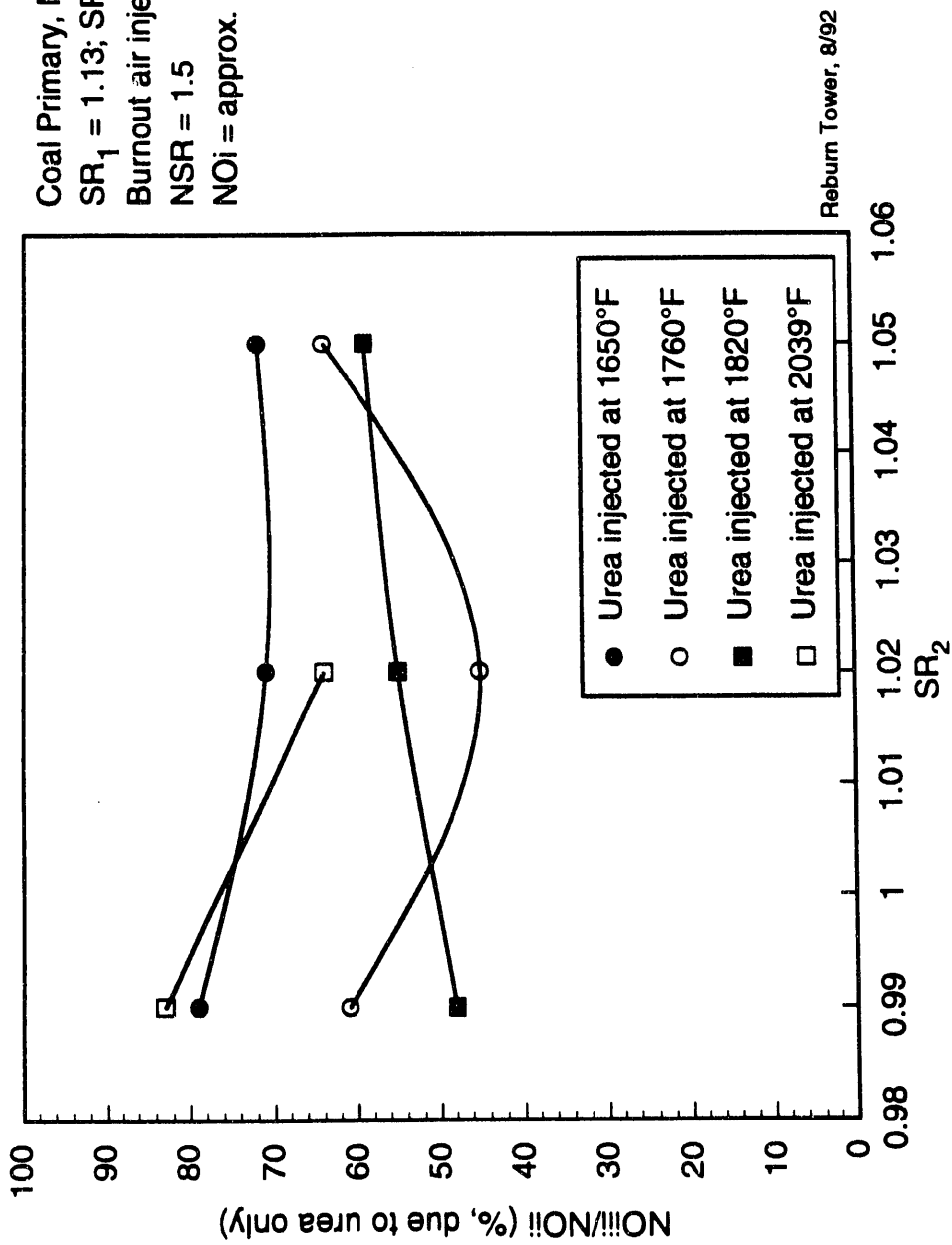


Figure 2-4. Effect of SR<sub>2</sub> and temperature on urea performance.

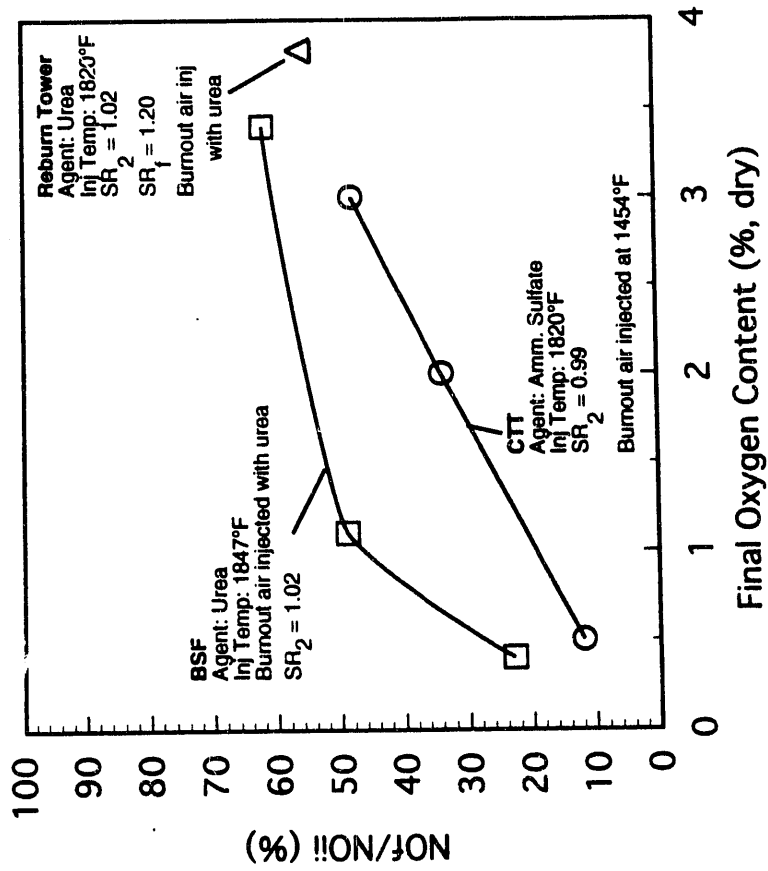


Figure 2-5. Effect of final oxygen content on urea performance.



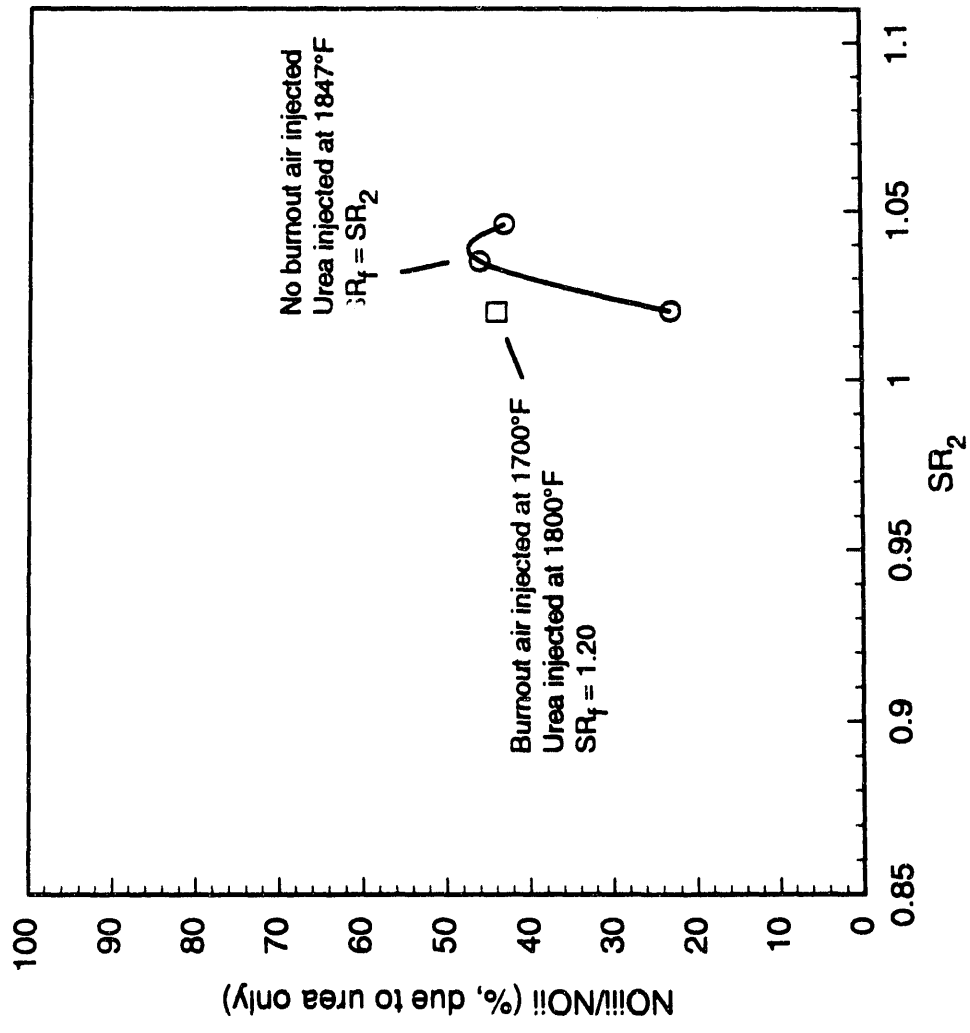


Figure 2-6. Effect of burnout air addition on urea performance at the BSF.

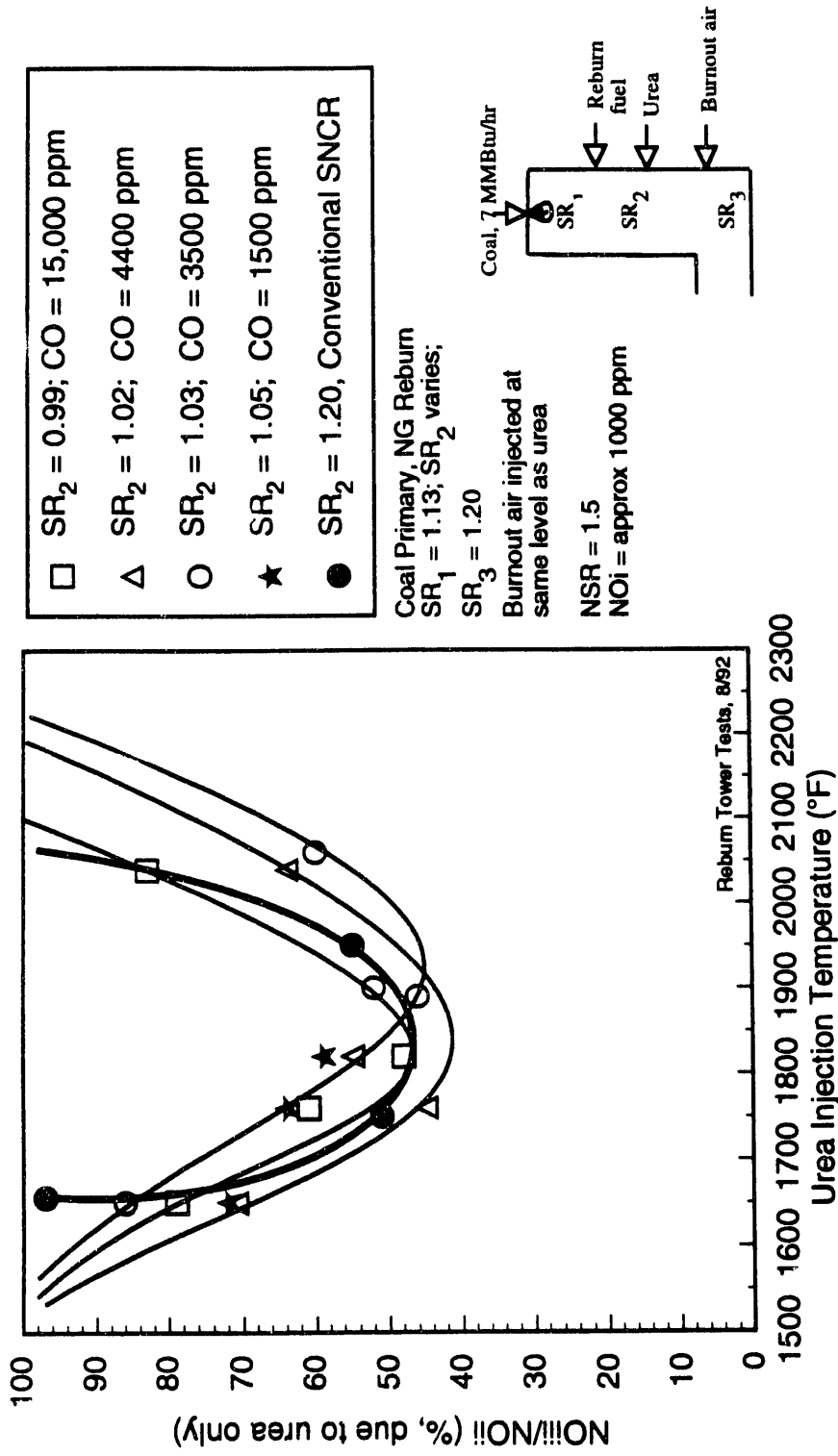


Figure 2-7. Effect of reburn zone stoichiometry on Advanced Reburning performance.

optimum injection temperatures, conventional SNCR performance is similar to that of the CO enhanced (via reburning) performance. This is probably due to the strong influence of final stoichiometry, since final stoichiometry is the same for all cases. However, the width of the temperature window appears to be affected by the reburn zone stoichiometry. Figure 2-8 details how the temperature window breadth is influenced by  $SR_2$ . Displayed is the temperature range "breadth" in which NO<sub>f</sub>/NO<sub>i</sub> is 60 percent or lower, plotted as a function of  $SR_2$ . At a stoichiometry of 1.02, the window is broader than other stoichiometries, achieving NO<sub>f</sub>/NO<sub>i</sub> of 60 percent or lower for a temperature range of 340°F. Conventional SNCR achieved NO<sub>f</sub>/NO<sub>i</sub> of 60 percent and lower for a temperature range of 265°F.

N<sub>2</sub>O formation was also studied as the reburn zone stoichiometry was varied. Figure 2-9 shows, again, that N<sub>2</sub>O emissions are highest at temperatures where urea performance is best. Figure 2-10 shows the same data with  $SR_2$  on the x-axis. This figure indicates that there is no distinct trend between  $SR_2$  and N<sub>2</sub>O formation. This lack of trend may be attributed to the high final stoichiometry that is achieved. If the  $SR_2$  influence on NO reduction becomes ambiguous with the addition of burnout air, it is possible that the  $SR_2$  influence on N<sub>2</sub>O formation also becomes ambiguous.

It was of interest to see how much of the reduced NO was being converted to N<sub>2</sub>O. Figure 2-11 shows  $\Delta N_2O/\Delta NO$  as a result of urea injection. From the figure it appears as if N<sub>2</sub>O is more likely to be produced on the cooler side of the temperature window. However, it is believed that this apparent increase in N<sub>2</sub>O production is actually a lack of N<sub>2</sub>O decomposition; N<sub>2</sub>O decomposes faster at higher temperatures and fails to decompose completely at cooler temperatures. Figure 2-12 shows the same data as a function of  $SR_2$ . As determined from Figure 2-9, N<sub>2</sub>O formation does not seem to be affected by reburn zone stoichiometry, when final stoichiometry is constant at 1.20.

### 2.3 Effect of Burnout Air Injection Location

The injection of burnout air completes the Advanced Reburning process. Burnout air can be added with the urea or downstream of the urea. Figure 2-13 compares the affect of burnout location on urea performance at all three pilot-scale facilities. CTT data indicate that there is an optimum burnout air injection temperature, shown in Figure 2-13 to be 1400°F. The theory behind this trend

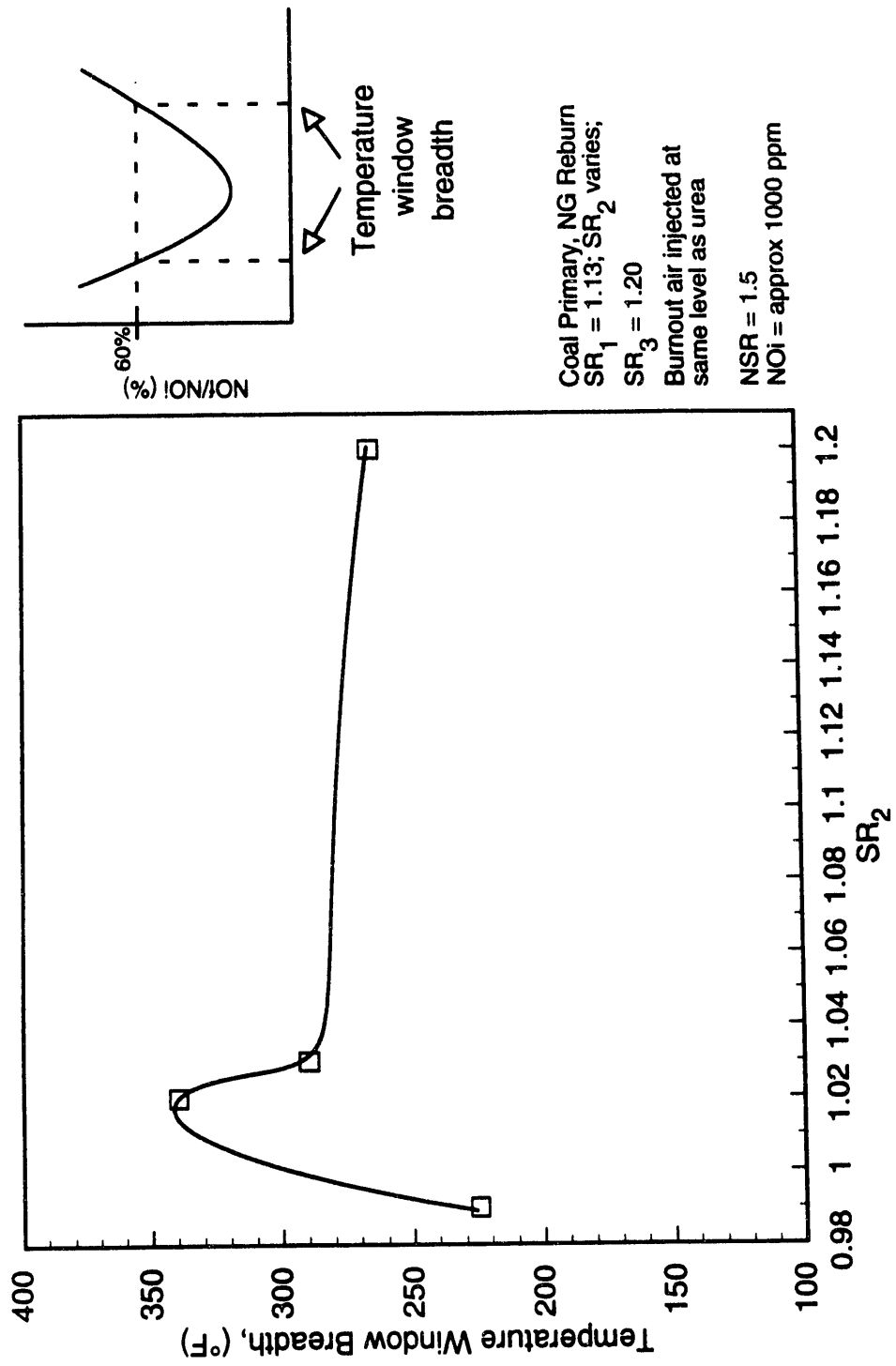


Figure 2-8. Temperature window breadth below NO<sub>x</sub>/NO<sub>x</sub> = 60% as a function of SR<sub>2</sub> at Reburn Tower.

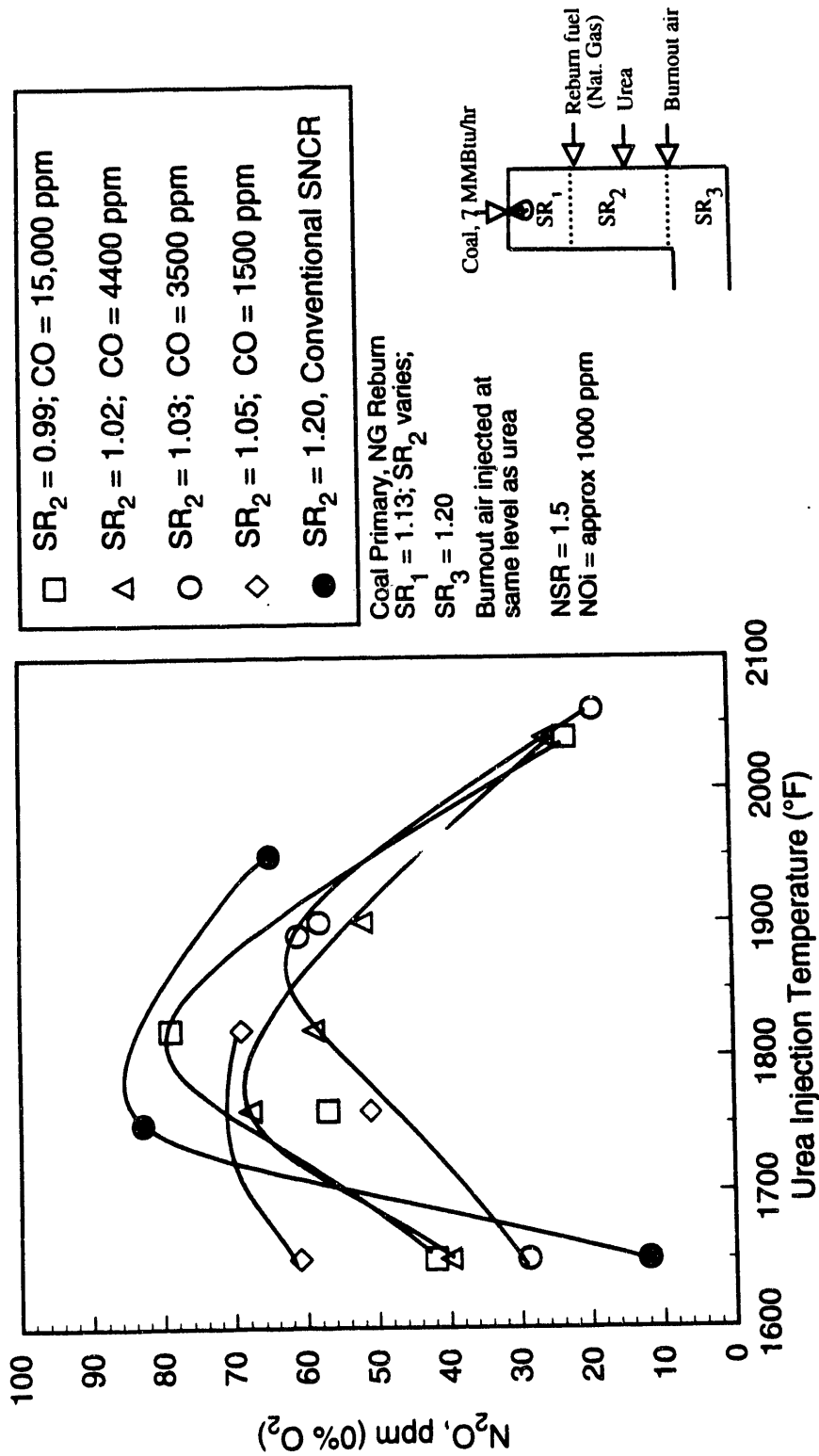


Figure 2-9. Effect of reburn zone stoichiometry on  $N_2O$  emissions.

Coal Primary, NG Reburn  
 SR<sub>1</sub> = 1.13; SR<sub>2</sub> varies;  
 SR<sub>3</sub> = 1.20  
 Burnout air injected at  
 same level as urea  
 NSR = 1.5  
 NOi = approx 1000 ppm

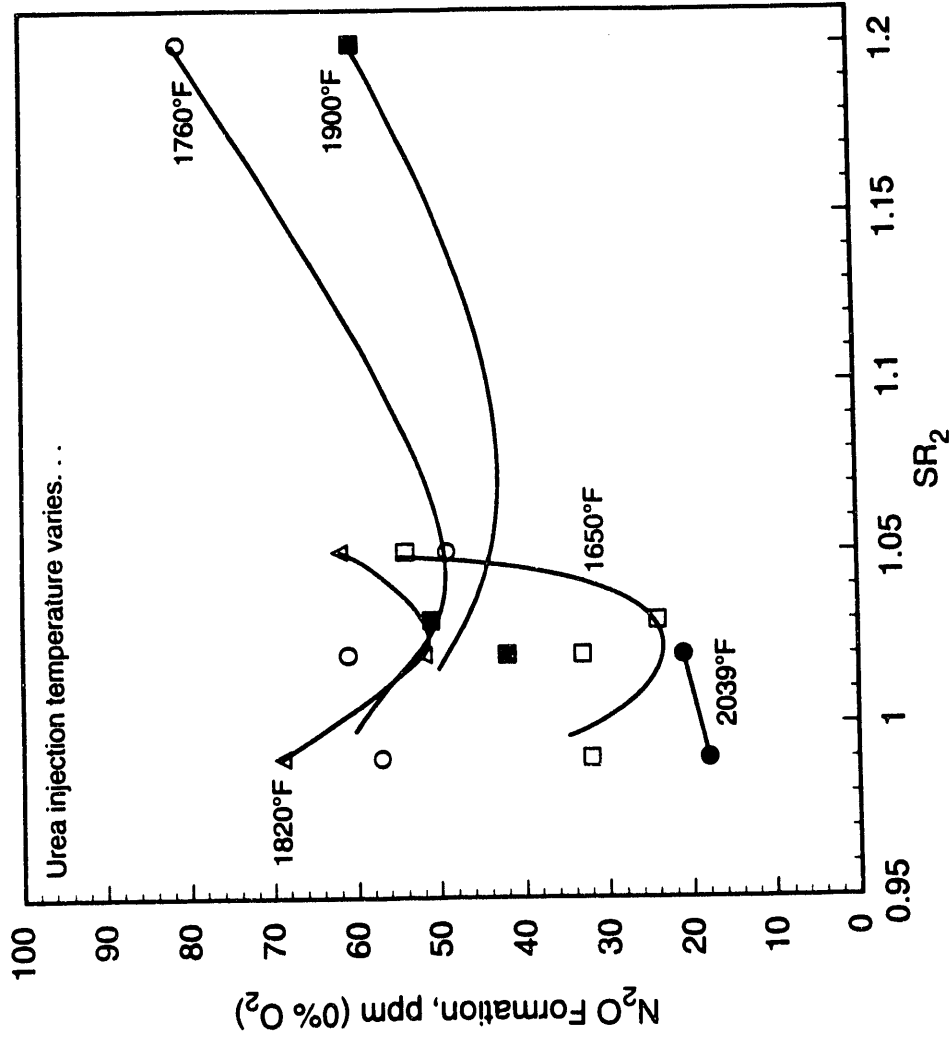


Figure 2-10. N<sub>2</sub>O formation as a function of SR<sub>2</sub> and urea injection temperature.

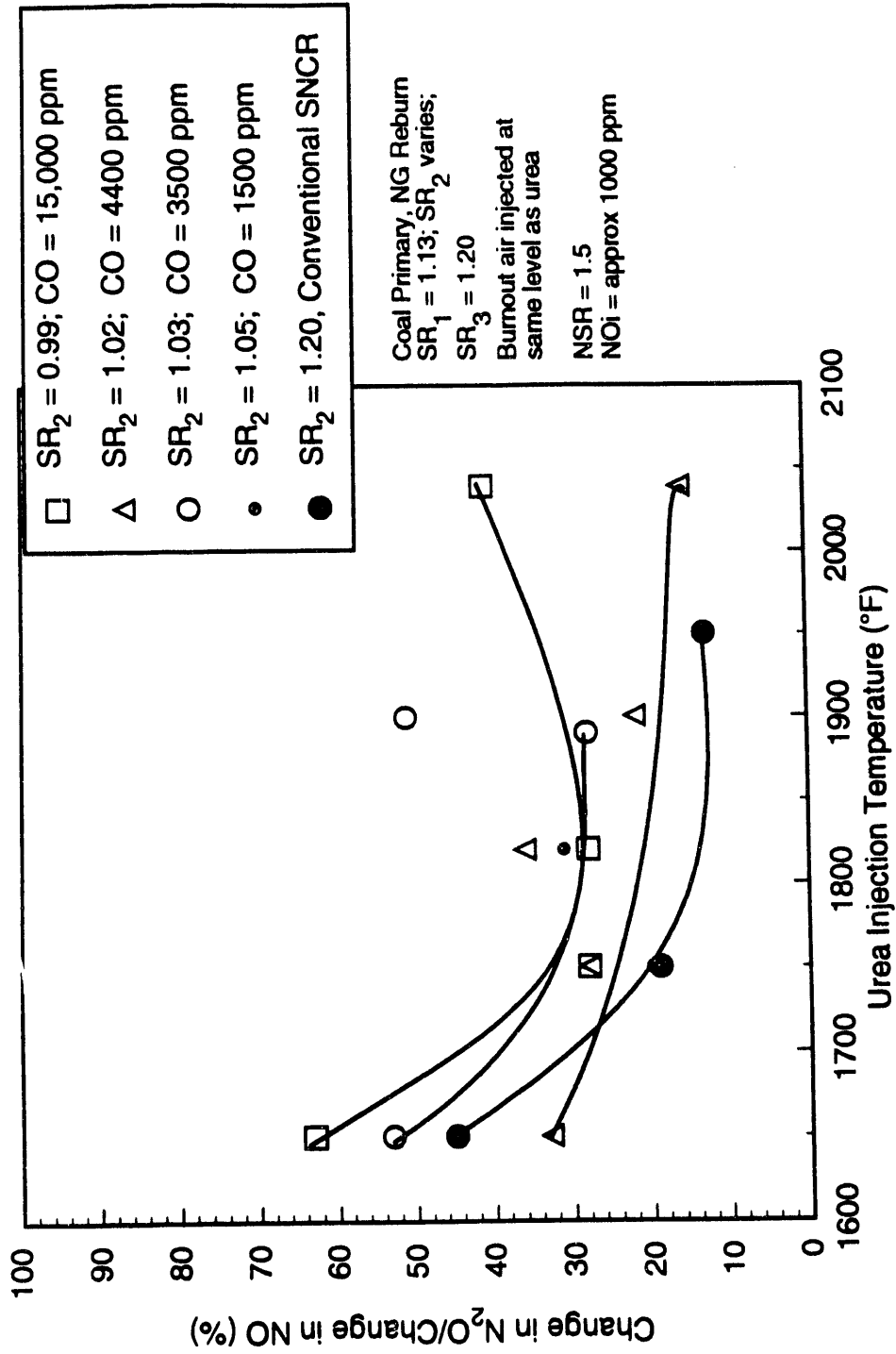


Figure 2-11.  $N_2O$  formation as a result of NO reduction.

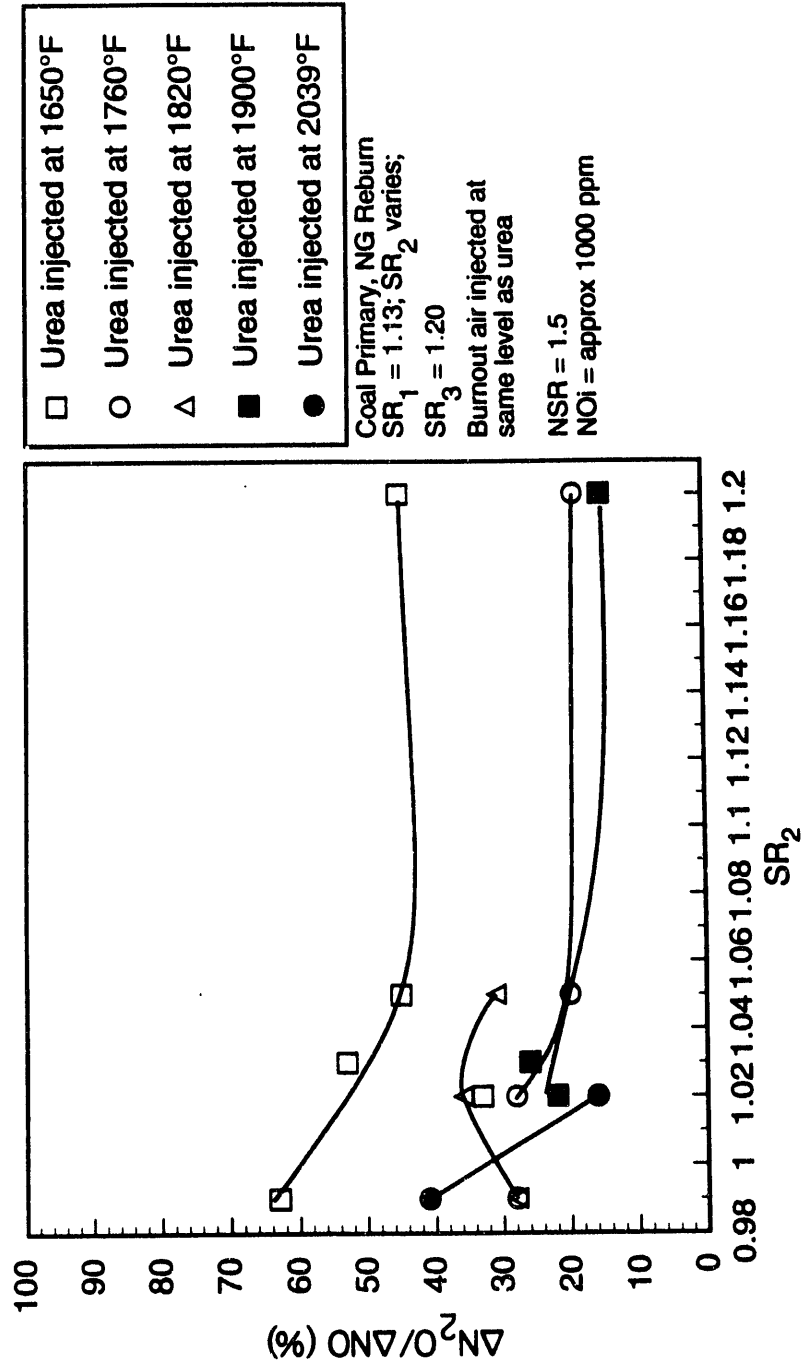


Figure 2-12.  $N_2O$  formation as a function of reburn zone stoichiometry and NO reduction.



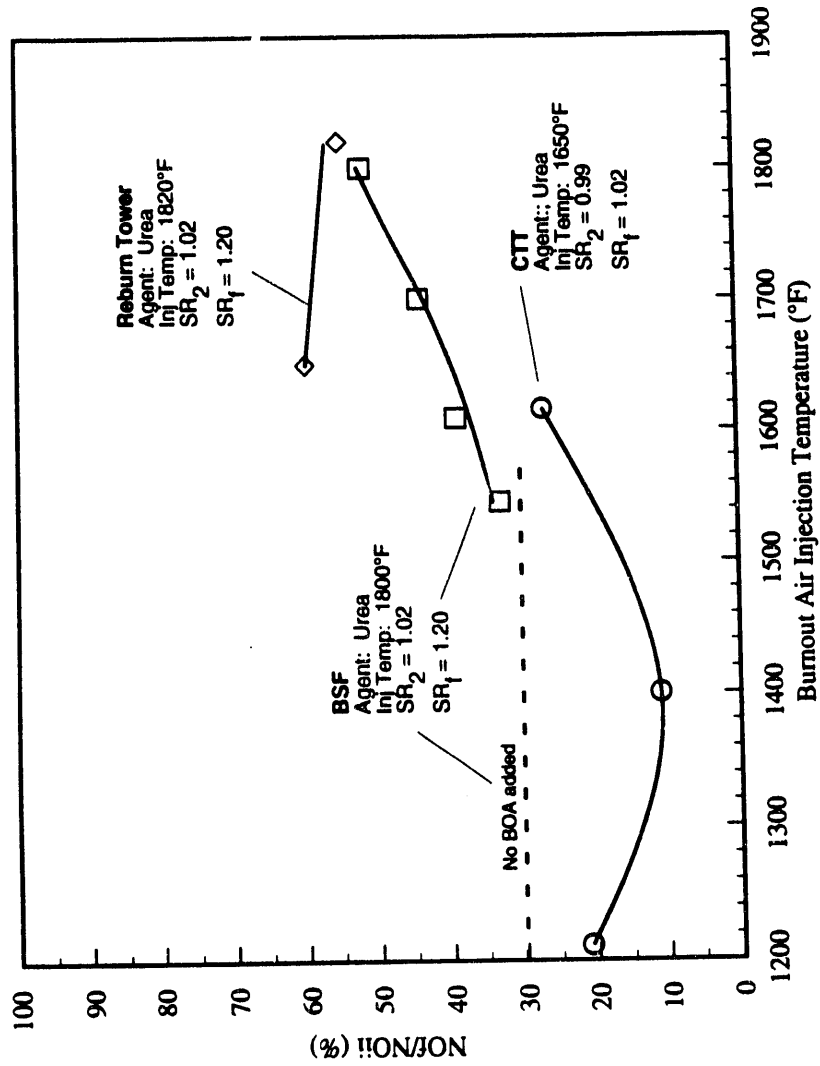


Figure 2-13. Effect of burnout air injection location on urea performance.

is that when the urea is injected in a uniformly fuel rich environment, it will not react until burnout air is injected. Accordingly, the temperature at which the burnout air is injected governs the rate of the deNO<sub>x</sub> reactions, hence the NO<sub>x</sub> reduction. If the air is injected too hot, the de NO<sub>x</sub> reactions will proceed more quickly than is optimum and NH<sub>2</sub> will be oxidized rather than allowed to reduce NO. If injected too cold, the deNO<sub>x</sub> reactions will not proceed.

BSF results indicate a similar trend. Here it was concluded that when the burnout air was injected far away from the urea injection point, performance improved. Burnout air addition brings with it an overabundance of radicals, capable of oxidizing NH<sub>2</sub> to NO, and therefore reducing performance. When the burnout air is injected cooler, oxidation of the NH<sub>2</sub> to NO is slower, and performance improves.

The dashed line in Figure 2-13 shows performance at the BSF when no burnout air was added. Good reduction was still achieved without the aid of burnout air addition. At the CTT, burnout air was required to complete the urea reactions. This difference in performance is probably due to the uniformity of the gases within the furnaces. Since the CTT is more uniformly fuel rich, with no O<sub>2</sub> present, urea reactions are not able to proceed. However at the BSF, CO/O<sub>2</sub> pockets are believed to exist which supply enough O<sub>2</sub> for the urea to react.

During the Reburn Tower tests, burnout air was injected in two locations, with the urea and downstream at 1650°F. The results of these tests, as displayed in Figure 2-13, contradict both the CTT and BSF results. Injecting the burnout air downstream resulted in approximately the same performance as when co-injecting the burnout air with the urea. The potential explanation lies in the Tower's turbulent mixing. CO/O<sub>2</sub> pockets exist in all furnaces, and the size of these pockets decrease with improved mixing capabilities. At the Tower, these pockets are expected to be larger than at the BSF since the BSF is generally laminar flow. If the pockets are large enough, and mixing within the furnace is poor, then the addition of burnout air would go unnoticed. This would result in no measurable effect of burnout air injection location on NO<sub>x</sub> emissions.

#### 2.4 Effect of Injected Urea Concentration

Urea concentration was adjusted by varying the urea solution strength. This allowed an approximately constant urea solution flow rate which is necessary to minimize mixing effects.

Urea strength is measured as the ratio of moles of injected  $\text{NH}_2$  to moles of  $\text{NO}$  existing in the flue gas. This ratio is referred to as the Nitrogen Stoichiometric Ratio (NSR), and for these experiments was varied between the standard, 1.5, and 2.5. Advanced Reburning performance and  $\text{N}_2\text{O}$  formation were evaluated at these concentrations as the urea was injected at 1900 °F. Results are displayed in Figure 2-14.  $\text{NO}_x$  performance improved and  $\text{N}_2\text{O}$  emissions increased with increasing NSR, as expected. 26 and 30 percent of the reduced  $\text{NO}$  converted to  $\text{N}_2\text{O}$  for the NSR cases of 1.5 and 2.5, respectively.

## 2.5 Overall $\text{NO}_x$ Reduction for Advanced Reburning at the Reburn Tower

Figure 2-15 displays the overall Advanced Reburning performance at the Reburn Tower. Gas reburning alone contributed a 66 percent reduction in  $\text{NO}_x$  emissions. Advanced Reburning resulted in 82 percent  $\text{NO}_x$  reduction.

Coal Primary, NG RB  
 $SR_1 = 1.13$ ;  $SR_2 = 1.03$ ;  $SR_t = 1.20$   
 Burnout air injected at same level as urea.  
 $NO_i = \text{approx } 990 \text{ ppm}$   
 $NO_{ii} = 350 - 420 \text{ ppm}$

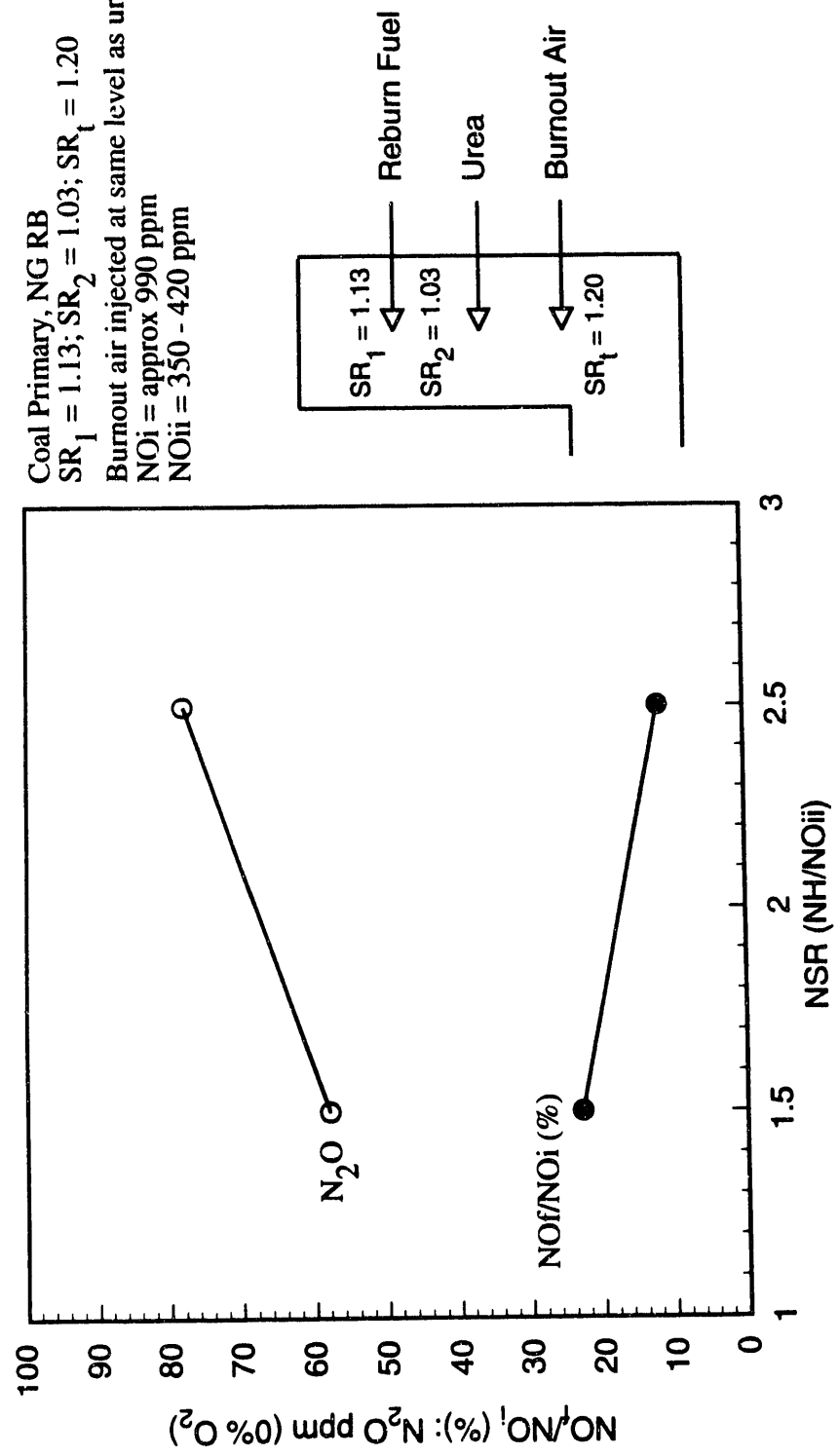


Figure 2-14. Effect of urea concentration on Advanced Reburning performance and by-product emissions.

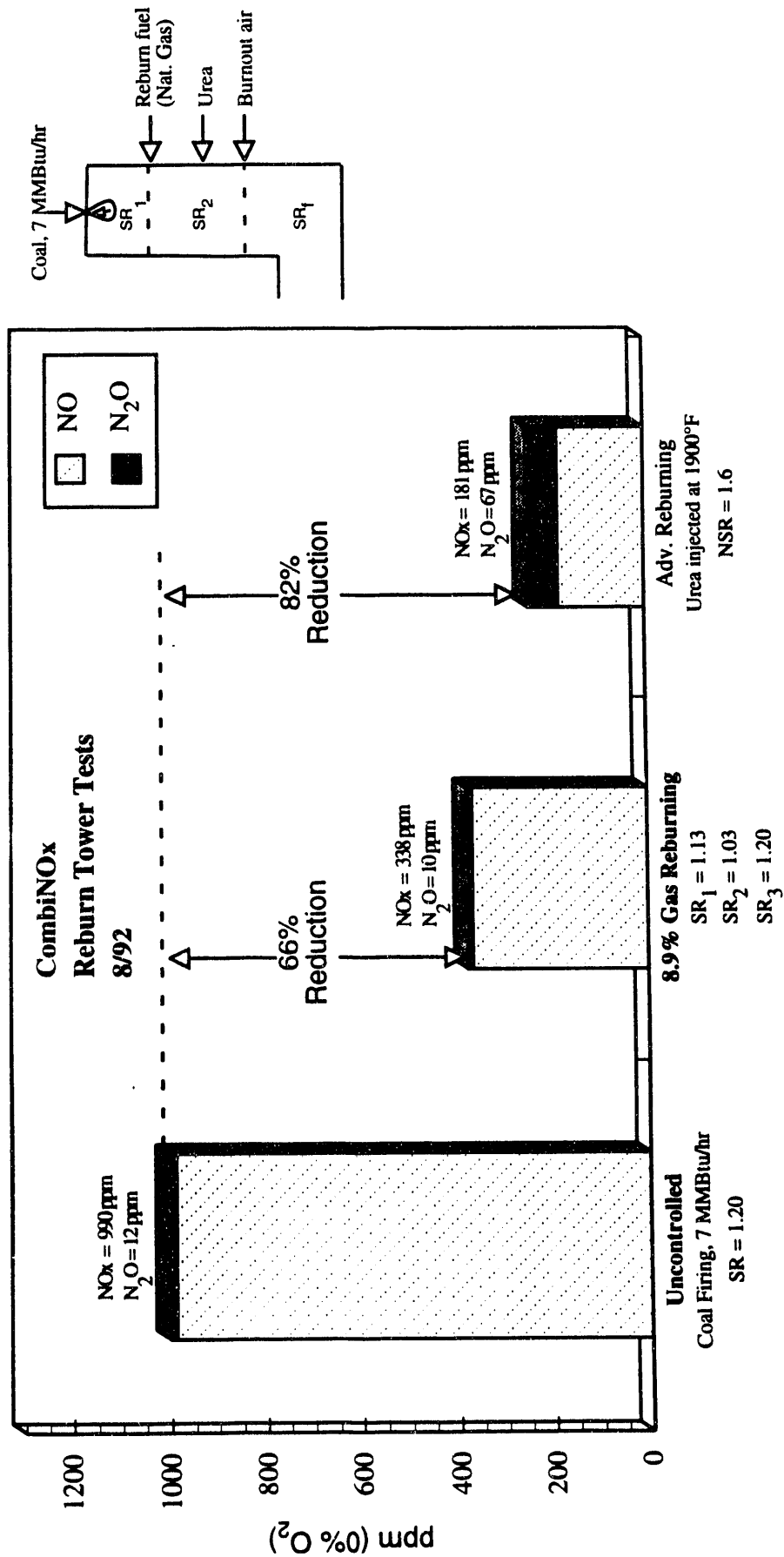
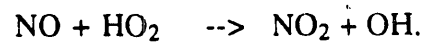
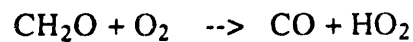
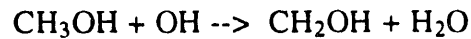


Figure 2-15. Overall CombiNO<sub>x</sub> performance at the Reburn Tower.

### 3.0 METHANOL INJECTION RESULTS

Methanol is injected downstream of the Advanced Reburning process to oxidize NO to NO<sub>2</sub>; NO<sub>2</sub> can then be removed in a wet-limestone scrubber. Based on previous kinetic modeling and Fundamental Phase bench-scale experiments, the reactions of interest are believed to be:



At the BSF, 82 percent oxidation of NO to NO<sub>2</sub> was achieved for natural gas-fired flue gas, but only 42 percent was achieved for coal. Even though a special sample conditioning system was devised to measure NO<sub>x</sub> when large quantities of NO<sub>2</sub> are present (details of the sample system can be found in Quarterly Report #5), it was hypothesized that both SO<sub>2</sub> and ash reacted in the system (there is evidence of both) to re-convert NO<sub>2</sub> to NO. This caused the coal-fired flue gas NO to NO<sub>2</sub> conversion efficiency appear to be lower than natural gas. At the Tower tests, an attempt was made to minimize these problems by keeping the water trap basic using a NaOH solution (this prevents SO<sub>2</sub> to SO<sub>3</sub> conversions, and therefore reduces NO<sub>2</sub> to NO conversions), and also by keeping all lines and filters clean of ash build-up.

During the Reburn Tower tests, methanol was injected by means of a single Spraying Systems, 180°, twin fluid nozzle, utilizing air as the atomization fluid. Methanol/NO ratio was varied between 2.1 and 4.4. Methanol was injected at 1150°F, which corresponds to the SWS inlet (displayed in Figure 1-2). NO/NO<sub>x</sub> measurements were taken at the SWS exit.

Figure 3-1 displays performance and N<sub>2</sub>O and CO formation as methanol concentration varies. Both NO and total NO<sub>x</sub> values are displayed, the difference of these measurements indicating the NO<sub>2</sub> formation that occurred as a result of methanol injection. Total NO<sub>x</sub> values are expected to stay constant, however a slight variation is detected. This variation may be attributed to changes in furnace conditions. During the experiments, oxygen levels varied slightly which would cause different NO<sub>x</sub> formation within the furnace.

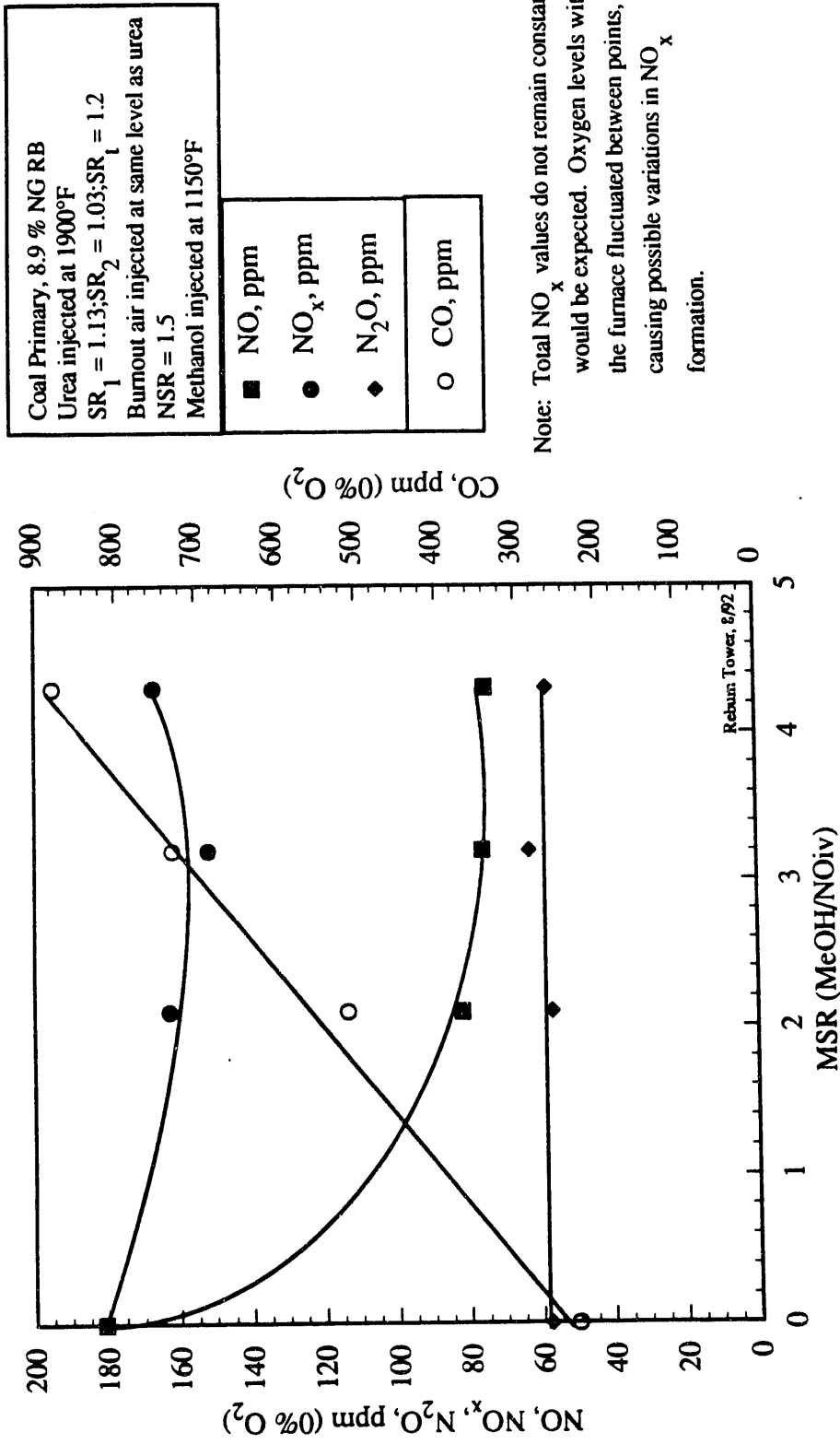


Figure 3-1. Effect of methanol concentration on performance and by-product formation.

At a methanol to NO ratio of 2.1, 55 percent of the NO oxidized to NO<sub>2</sub>, with little improvement in performance as the methanol concentration increased beyond this point. While this is an improvement over the BSF results (possibly attributable to the steps taken to minimize SO<sub>2</sub> and ash sampling interferences) the results are still not satisfactory. It is not understood why the coal-fired flue gas does not perform as well as the natural gas.

CO emissions continued to increase with increasing methanol concentration. The methanol chemistry shows that 1 mole of CO formation is expected to form for each mole of injected methanol. Depending upon injection temperature, the CO can oxidize to CO<sub>2</sub>. At an injection temperature of 1150°F, for each mole of injected methanol approximately 0.9 moles of CO were formed. This rate of CO formation indicates that the quantities of methanol injected should be minimized.

N<sub>2</sub>O emissions remained approximately constant throughout the methanol injection step of the CombiNO<sub>x</sub> process.

During the Reburn Tower tests it was observed that all of the newly formed NO<sub>2</sub> converted back to NO by the time the flue gas reached the baghouse. A series of NO/NO<sub>x</sub> measurements were taken at various locations throughout the back end of the furnace (Figure 3-2) to determine where the re-conversion was occurring. NO measurements were taken with a standard CEM sample conditioning system, under the assumption that with this system, NO measurements are acceptable but NO<sub>2</sub> measurements are inaccurate. One set of measurements was taken with the newly developed NO/NO<sub>x</sub> sampling system which is capable of accurately measuring high concentrations of NO<sub>2</sub>. Results were consistent between the sampling systems, showing that NO measurements increased as the sample probe was moved further and further downstream from the methanol injection point. This phenomena does not appear to be a sampling artifact since measurements were re-taken several times using more than one sampling system, and all results were consistent. Since thermodynamic equilibrium favors NO over NO<sub>2</sub> at high temperatures, a sampling error would tend to reflect larger NO measurements at the higher temperatures. Also, stainless steel is a known catalyst of NO<sub>2</sub> to NO reduction at higher temperatures. The stainless steel sampling probe (water-cooled) would be more likely to create artificially high NO measurements at high temperatures than at low temperatures. However, measurements consistently agreed that NO levels were larger at lower temperatures.



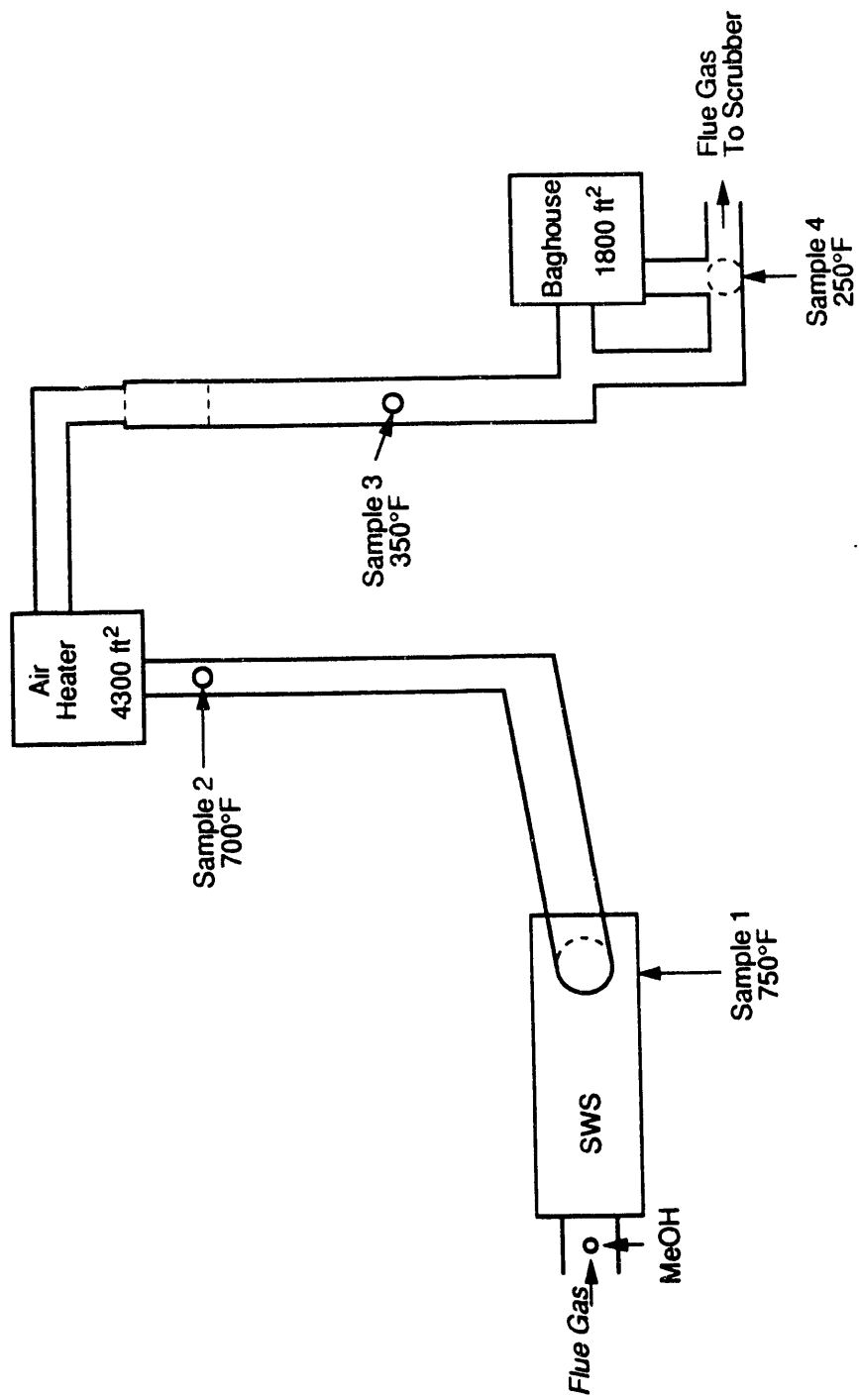


Figure 3-2. Reburn Tower sample ports for NO<sub>2</sub> to NO re-conversion.

Figure 3-3 shows how much re-conversion occurs within certain sections of the furnace. The measurement at sample port #1 (the SWS exit) was used as a reference point since NO<sub>2</sub> concentrations were still relatively high at this point. The figure shows how much of the NO<sub>2</sub> measured at sample port #1 had converted back to NO by the time the flue gas reached the air-heater entrance and baghouse locations. After the baghouse, 84 - 100 percent of the formed NO<sub>2</sub> had converted back to NO.

There has been speculation as to the cause of this re-conversion, however the exact cause has not been determined. Thermodynamic equilibrium favors the NO side of the reaction,



at temperatures above 700°F (shown in Figure 3-4). However, re-conversion continues to occur at temperatures below this, indicating there is a catalytic effect occurring that reduces NO<sub>2</sub> back to NO at cooler temperatures. Stainless steel has been shown to aid in the conversion of NO<sub>2</sub> to NO and small amounts of (mild) steel are present in the Tower. Coal ash has also been shown to reduce NO<sub>2</sub> to NO, but the furnace ducts were cleaned of collected ash and the re-conversions continued to occur. Fuels containing trace elements such as Vanadium had been burned previously at the Reburn Tower; it is possible that remains from these fuels are responsible for the re-conversions.

The re-conversion may also be an artifact of the very long residence times and slow quench rates at the Reburning Tower. Re-conversion is plotted as a function of residence time in Figure 3-5. Figure 3-6 compares the quench rates at the Tower with those of a full-scale boiler, Hennepin Station. It is possible that the faster quench rates typical of utility boilers will minimize re-conversion of NO<sub>2</sub> back to NO. Further experiments will be required to determine the exact cause of the re-conversion, and whether or not this re-conversion would happen on a full-scale facility. If these re-conversions are characteristic of the Reburn Tower only, then it is believed that reductions by methanol injection may be even better than those previously reported.

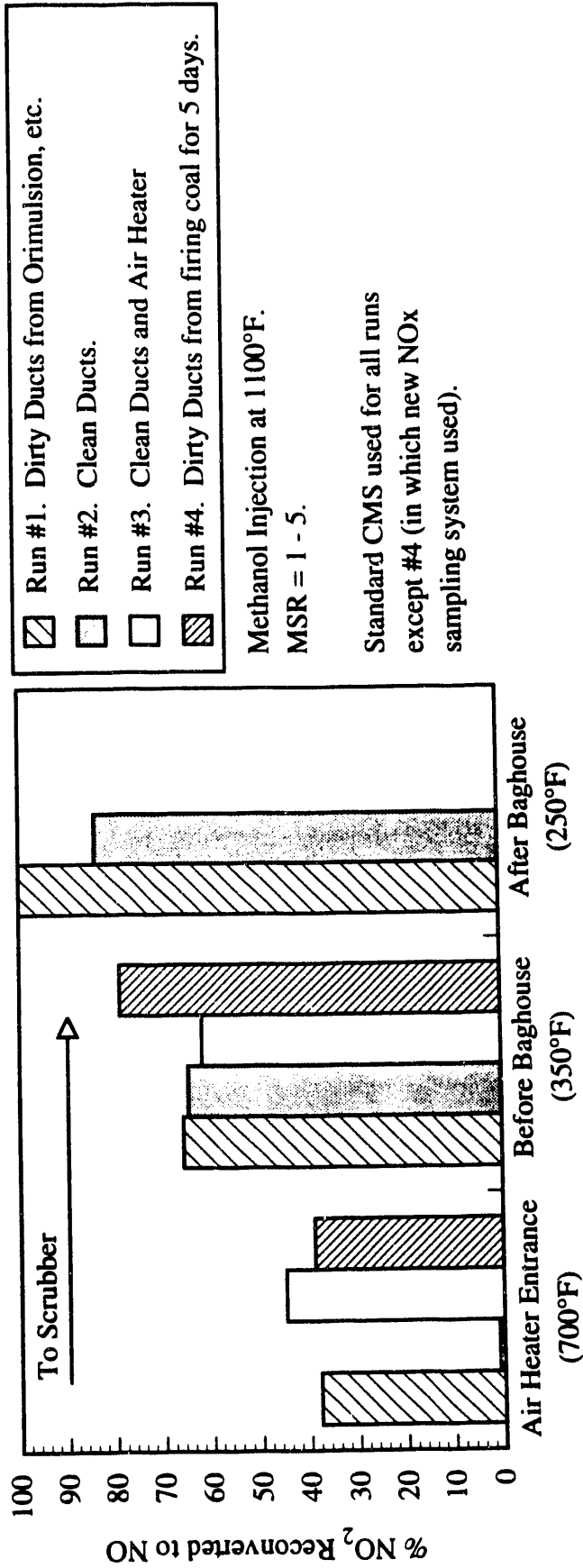


Figure 3-3. Reburn Tower NO<sub>2</sub> to NO Reconversion

Initial Concentrations:  
 CO<sub>2</sub> 5.868 lbmol  
 H<sub>2</sub>O 0.2775 lbmol  
 SO<sub>2</sub> 0.2775 lbmol  
 NO 50 ppm  
 NO<sub>2</sub> 50 ppm  
 N<sub>2</sub> 32.87 lbmol  
 O<sub>2</sub> 1.437 lbmol

Prediction assumes  
 equilibrium is reached.

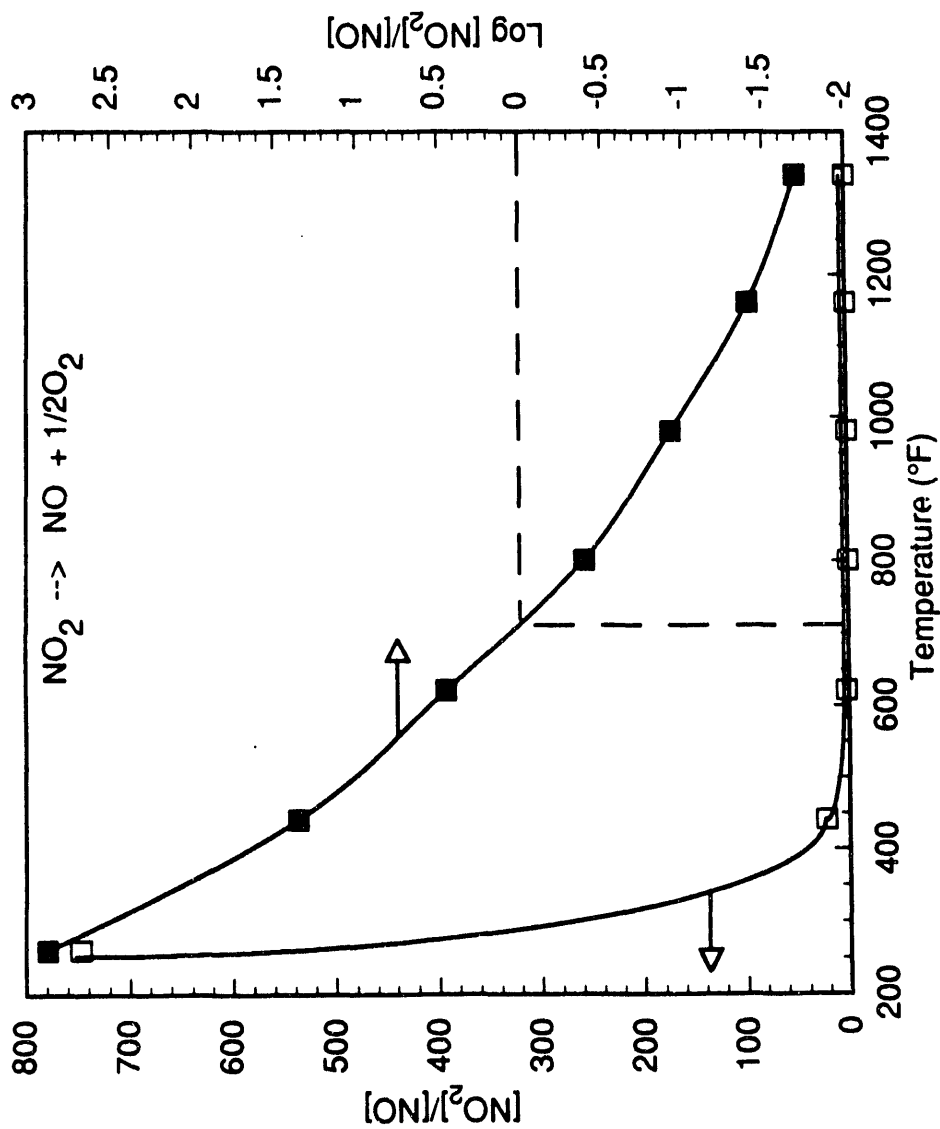


Figure 3-4. NASA equilibrium model results.

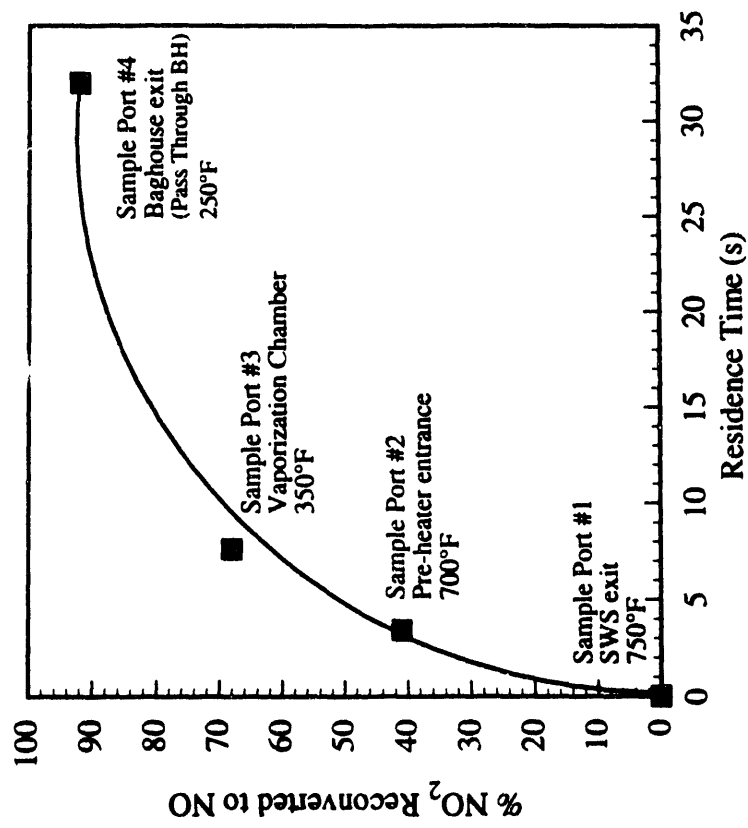


Figure 3-5. Effect of residence time on NO<sub>2</sub> to NO re-conversion.

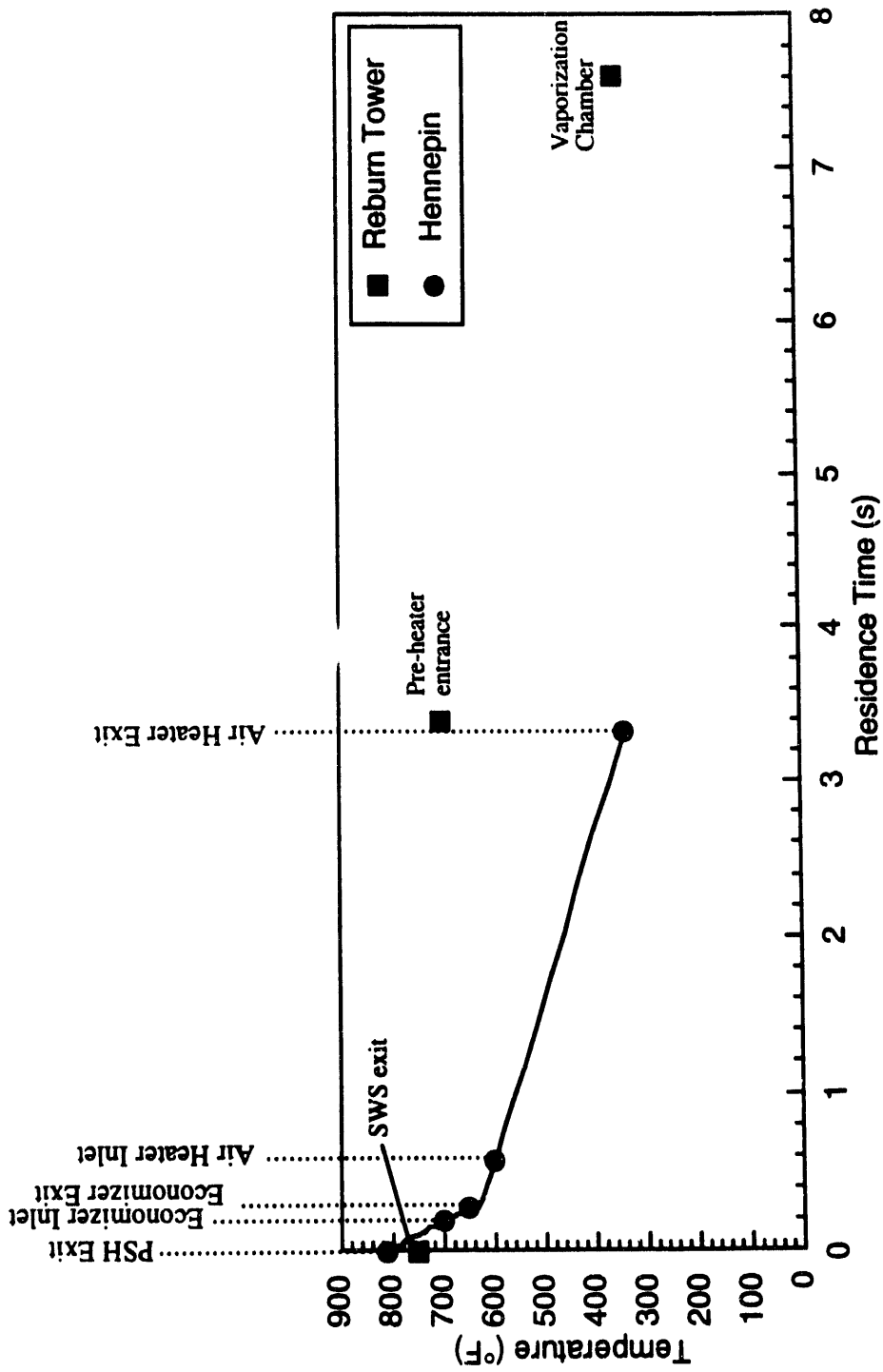


Figure 3-6. Quench rate comparison between Reburn Tower and full-scale, Hennepin Station.

## 4.0 PILOT-SCALE SCRUBBING STUDIES RESULTS

The final step of the CombiNO<sub>x</sub> process is the removal of the NO<sub>2</sub> from the flue gas using a modified wet-limestone scrubbing procedure. Bench-scale experiments and kinetic modeling have been performed to evaluate the process and determine a scrubbing solution that is capable of efficiently removing NO<sub>2</sub> and SO<sub>2</sub> simultaneously. These studies produced a scrubbing slurry consisting of a combination of calcium carbonate (CaCO<sub>3</sub>), sodium carbonate (Na<sub>2</sub>CO<sub>3</sub>), and sodium thiosulfate (Na<sub>2</sub>S<sub>2</sub>O<sub>3</sub>). CaCO<sub>3</sub> (also known as limestone) supplies the Ca needed for calcium sulfite and calcium sulfate precipitation, and thus removal of sulfur from the flue gas. However, the sulfite ion is necessary for NO<sub>2</sub> removal, therefore it is not desirable to precipitate all of the sulfite ions with the calcium. It has been proposed that the ratio of carbonate to sulfite ions is constant throughout the majority of the scrubbing process. Na<sub>2</sub>CO<sub>3</sub> supplies carbonate ions without supplying the precipitating calcium, therefore sustaining the concentration of sulfite ion in solution. Na<sub>2</sub>S<sub>2</sub>O<sub>3</sub> is added to the solution to inhibit oxidation of sulfite to sulfate. This modified slurry removed 99+ percent SO<sub>2</sub> and 95 percent NO<sub>2</sub> from a simulated flue gas at the bench-scale level. Presented here are the results from scale-up experiments performed at 2 pilot-scale facilities.

### 4.1 Small Pilot-Scale NO<sub>2</sub> Scrubbing Results

Research Cottrell was sub-contracted to study the effect of several operating parameters on the scrubbing efficiency of the newly developed slurry. Their facility, displayed in Figure 4-1, consists of a propane combustor, 16 inch diameter and 20 feet high absorber tower, absorber feed tank, analytical train, and solid disposal system. The 0.35 million Btu/hr propane combustor exhaust was doped with SO<sub>2</sub> and NO<sub>2</sub> to simulate a coal-fired flue gas. The simulated flue gas entered the tower from the bottom, traveled through five sections to the top, and exited to the gas sample conditioning systems and analyzers. The first two sections were packed with a light material to provide improved gas/liquid contact. Measurements of NO<sub>x</sub>, SO<sub>2</sub>, CO, and O<sub>2</sub> in the flue gas were made at the entrance of the absorber tower, while NO<sub>x</sub> and SO<sub>2</sub> measurements were made at the exit. The scrubber slurry was continually mixed with dry limestone, sodium salts, and water in the absorber feed tank. From the feed tank, the slurry was pumped to the top of the absorber tower and dispensed in counter flow to the flue gas with a single slurry nozzle. The slurry solution was drained by gravity from the bottom of the tower back to the feed tank.

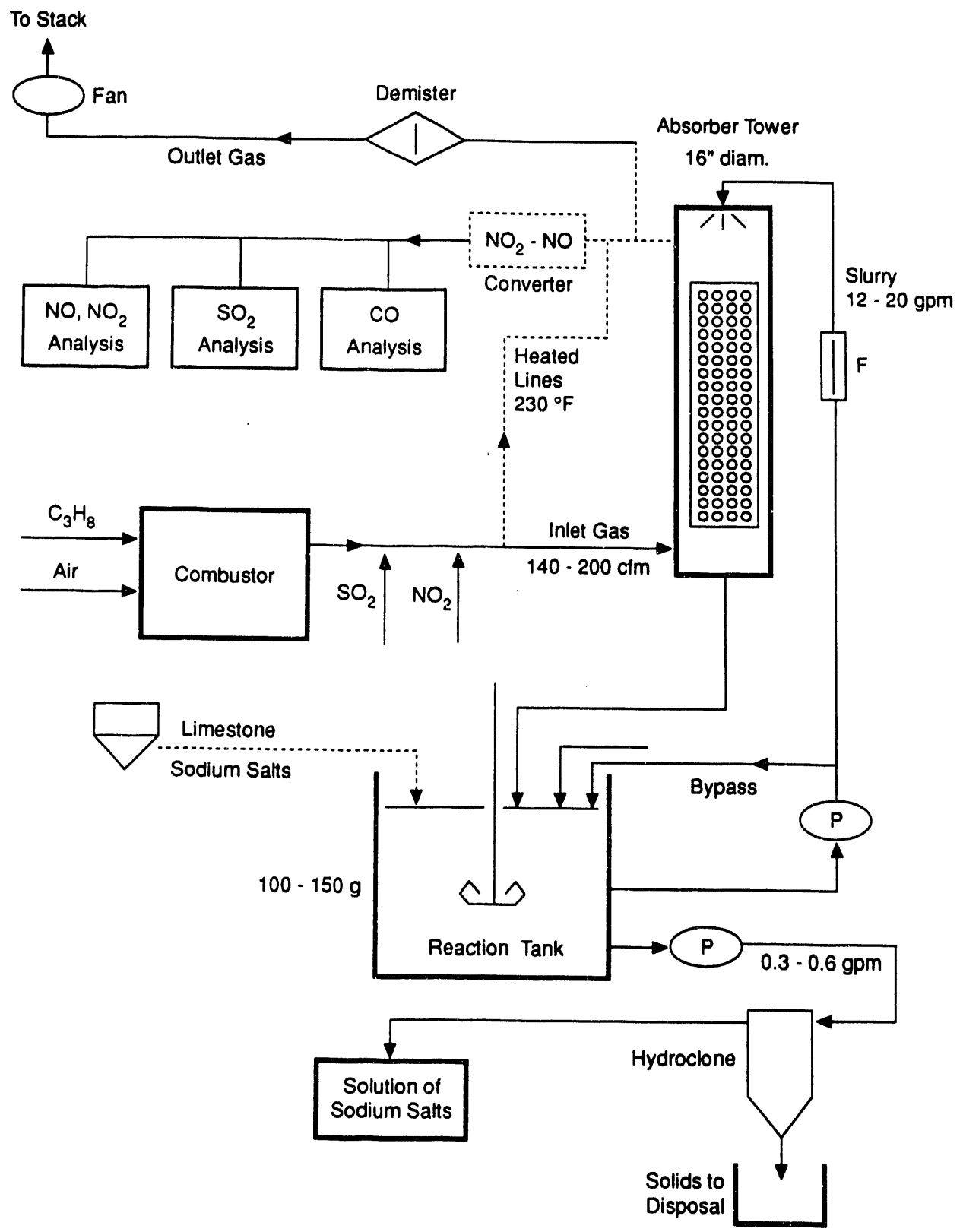


Figure 4-1. Research Cottrell pilot-scale scrubbing apparatus.



Simultaneous scrubbing of NO<sub>2</sub> and SO<sub>2</sub> was evaluated using scrubbing salts consisting of 49.5 percent CaCO<sub>3</sub>, 49.5 percent Na<sub>2</sub>CO<sub>3</sub>, 1 percent Na<sub>2</sub>S<sub>2</sub>O<sub>3</sub>. During this test series, the following parameters were varied: liquid/gas ratio (liquid flow and gas flow were independently varied), initial NO<sub>2</sub> concentration, concentration of sodium carbonate in slurry, and concentration of sodium thiosulfate in slurry.

The ratio of slurry flow rate to flue gas flow rate is defined as the liquid to gas ratio (L/G), and is expressed here in units of (gallons of slurry)/(1000 cubic feet of gas). The slurry flow and gas flow were varied independently of one another. Figure 4-2 summarizes the effects of L/G ratio on NO<sub>2</sub> scrubbing efficiency. As would be expected, a larger L/G ratio produces better NO<sub>2</sub> removal. Even though not depicted in the figure, data indicate that gas flow rate has a larger affect on the NO<sub>2</sub> scrubbing efficiency than slurry flow rate. By decreasing the gas flow rate by a small fraction (from 135 to 115 cfm), efficiency increased from 77 to 84 percent. However, when the slurry flow rate was nearly doubled (11.4 to 20 gpm), the efficiency only increased by approximately the same amount, 77 to 85 percent.

Research Cottrell also performed experiments to determine the effect of initial NO<sub>2</sub> concentration on NO<sub>2</sub> scrubbing efficiency. Slurry flow rate remained approximately constant as inlet NO<sub>2</sub> concentration was varied by adjusting the doping gas flow rate. Results are displayed in Figure 4-3. The general trend shows that scrubbing effectiveness dropped as initial NO<sub>2</sub> concentrations increased.

The effect of Na<sub>2</sub>CO<sub>3</sub> concentration on NO<sub>2</sub> and SO<sub>2</sub> scrubbing efficiency was evaluated by diluting the scrubbing solution by a factor of two, while continuing to add limestone to maintain pH and ion concentration. Figure 4-4 shows that even though scrubbing efficiency was initially hampered by the dilution that occurs 200 minutes into the test, with time the NO<sub>2</sub> removal efficiency rose again to approximately the same level as before the dilution. Even after diluting the slurry a second time, the NO<sub>2</sub> scrubbing efficiency returned to almost the original value. These data indicate that NO<sub>2</sub> removal efficiency is not sensitive to Na<sub>2</sub>CO<sub>3</sub> concentration in this range.

The effect of sodium thiosulfate concentration was tested by adding an additional 3.8 mmol of sodium thiosulfate per liter of solution. NO<sub>2</sub> removal efficiency jumped from 65 percent to 89-90 percent within 15 minutes, and SO<sub>2</sub> removal efficiency remained at 99+ percent. The thiosulfate

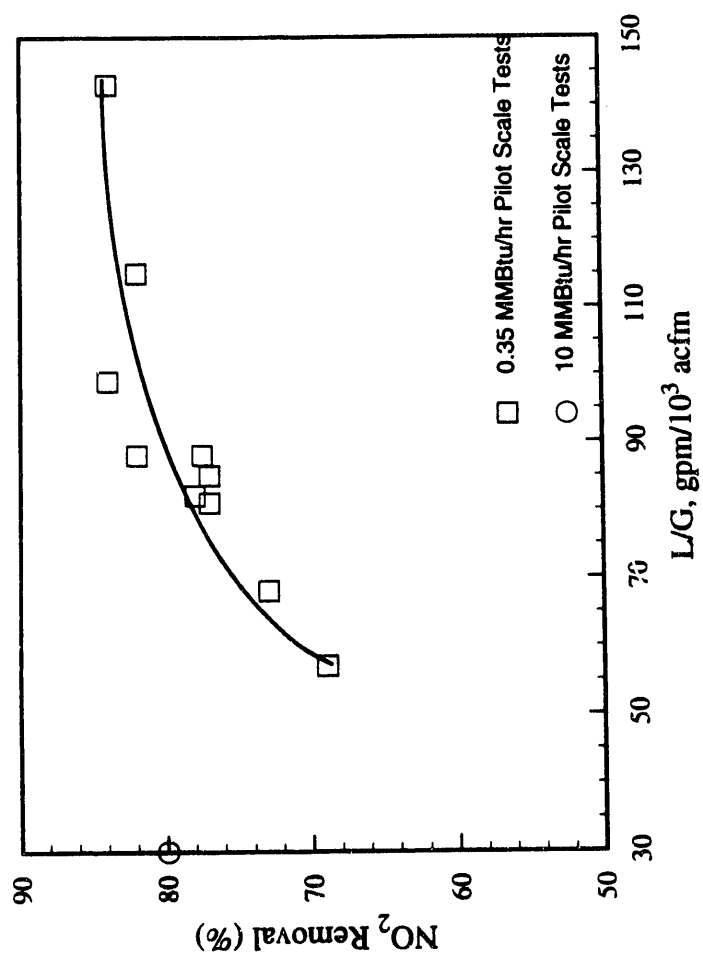


Figure 4-2. Effect of liquid to gas ratio on NO<sub>2</sub> scrubbing efficiency.

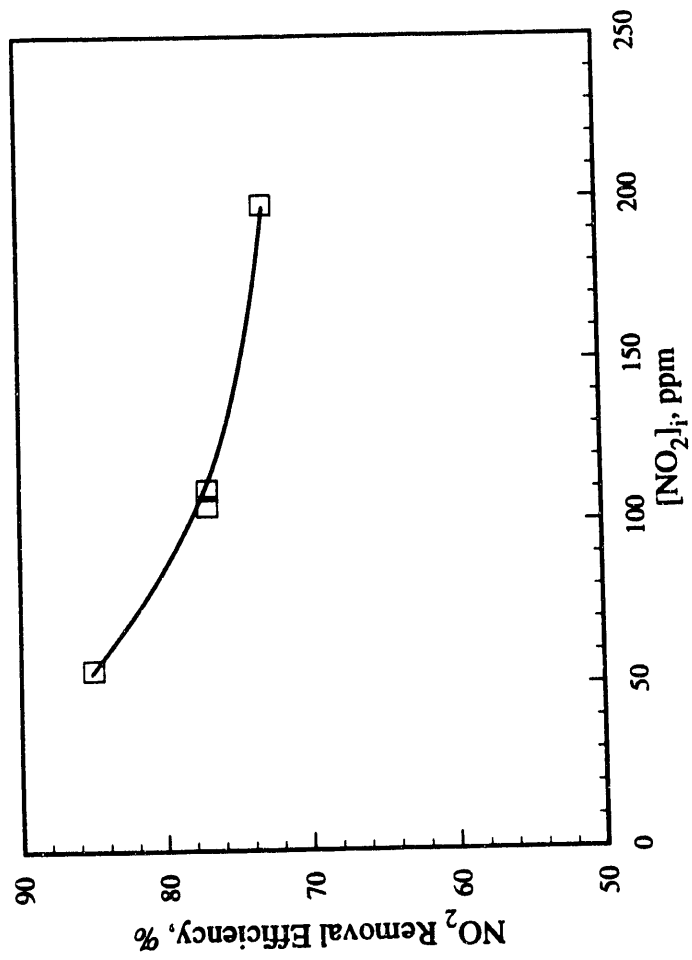


Figure 4-3. Effect of initial NO<sub>2</sub> concentration on NO<sub>2</sub> removal efficiency.

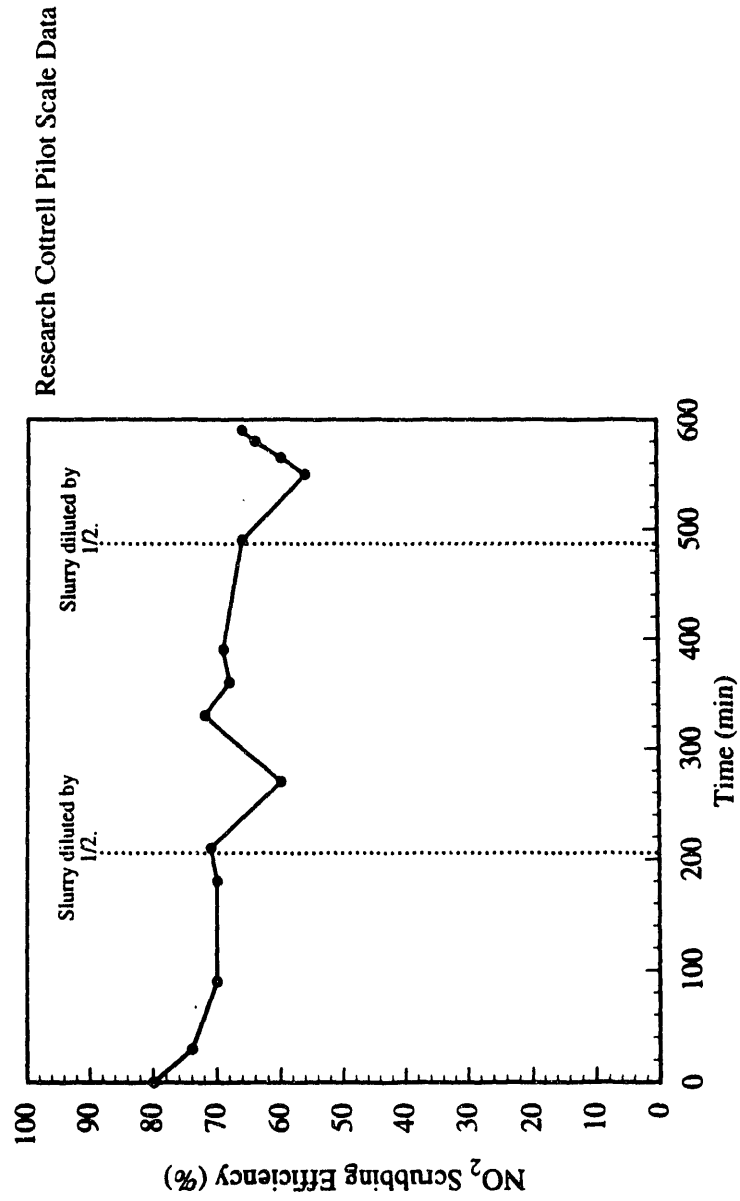


Figure 4-4. Effect of Na<sub>2</sub>CO<sub>3</sub> dilution on NO<sub>2</sub> scrubbing performance.

inhibits oxidation of sulfite to sulfate, sustaining the presence of sufficient sulfite ions for NO<sub>2</sub> capture.

Throughout the experiments discussed above, scrubbing solution composition measurements were periodically taken. During model and bench-scale studies, it was observed that the scrubber reactions proceeded in three stages. During the first stage, carbonate ion concentration falls while the concentrations of sulfate, bisulfate and sulfite ions increase. This first stage ends when the ratio of carbonate to sulfite ion becomes so low that calcium carbonate starts to dissolve while calcium sulfite precipitates. During this second stage the ratio of the concentrations of carbonate and sulfite ion is constant and the pH remains fairly steady. The concentration of sulfate ion increases until calcium sulfate starts to precipitate. The second stage ends when the calcium carbonate is exhausted. When this happens, the pH begins to rise until it reaches a level at which SO<sub>2</sub> absorption fails and scrubbing solution is spent. Pilot-scale slurry samples indicate that the scrubber operates in the second stage, and this stage can be sustained with the addition of solution salts. Pilot-scale studies also show that sulfite to sulfate oxidation occurs at a rate much faster than that predicted by the model, for this reason, larger concentrations of sodium thiosulfate than initially recommended may be beneficial to the scrubbing process.

#### 4.2 Large Pilot-Scale NO<sub>2</sub> Scrubbing Results

A single scrubbing test was performed in EER's large pilot-scale facility. The large pilot-scale scrubber facility consisted of a spray tower 6 feet in diameter and 16 ft high, with an array of 16 nozzles. Natural gas combustion products were doped with NO<sub>2</sub> to a concentration of 74 ppm. SO<sub>2</sub> was not added. The test was conducted at an L/G ratio of approximately 30 gal/1000 acf and the scrubbing solution was 9 percent CaCO<sub>3</sub>, 9 percent NaOH, 1 percent Na<sub>2</sub>S<sub>2</sub>O<sub>3</sub>. The test results are compared to the small-scale results as a function of L/G ratio in Figure 4-2. Much higher NO<sub>2</sub> removal was achieved than was expected based on the small pilot-scale results. This may be due to the higher concentration of sodium thiosulfate used in the large pilot-scale test, especially since higher concentrations of sodium thiosulfate may be required than previously believed. However, additional tests are necessary to validate this hypothesis.

## 5.0 SUMMARY

The complete CombiNO<sub>x</sub> process has now been demonstrated at a level that is believed to be representative of a full-scale boiler in terms of mixing capabilities. A summary of the results is displayed in Figure 5-1. While firing Illinois Coal on the Reburn Tower, Advanced Reburning was capable of reducing NO<sub>x</sub> by 83 percent. The injection of methanol oxidized 50 - 58 percent of the existing NO to NO<sub>2</sub>. Assuming that 85 percent of the newly formed NO<sub>2</sub> can be scrubbed in a liquor modified wet-limestone scrubber, the CombiNO<sub>x</sub> process has been shown capable of reducing NO<sub>x</sub> by 90 - 91 percent in a large pilot-scale coal-fired furnace. There is still uncertainty regarding the fate of the NO<sub>2</sub> formed with methanol injection. Tests should be conducted to determine whether the reversion is thermodynamic or catalytic, and what steps can be taken (such as quench rate) to prevent it from happening.

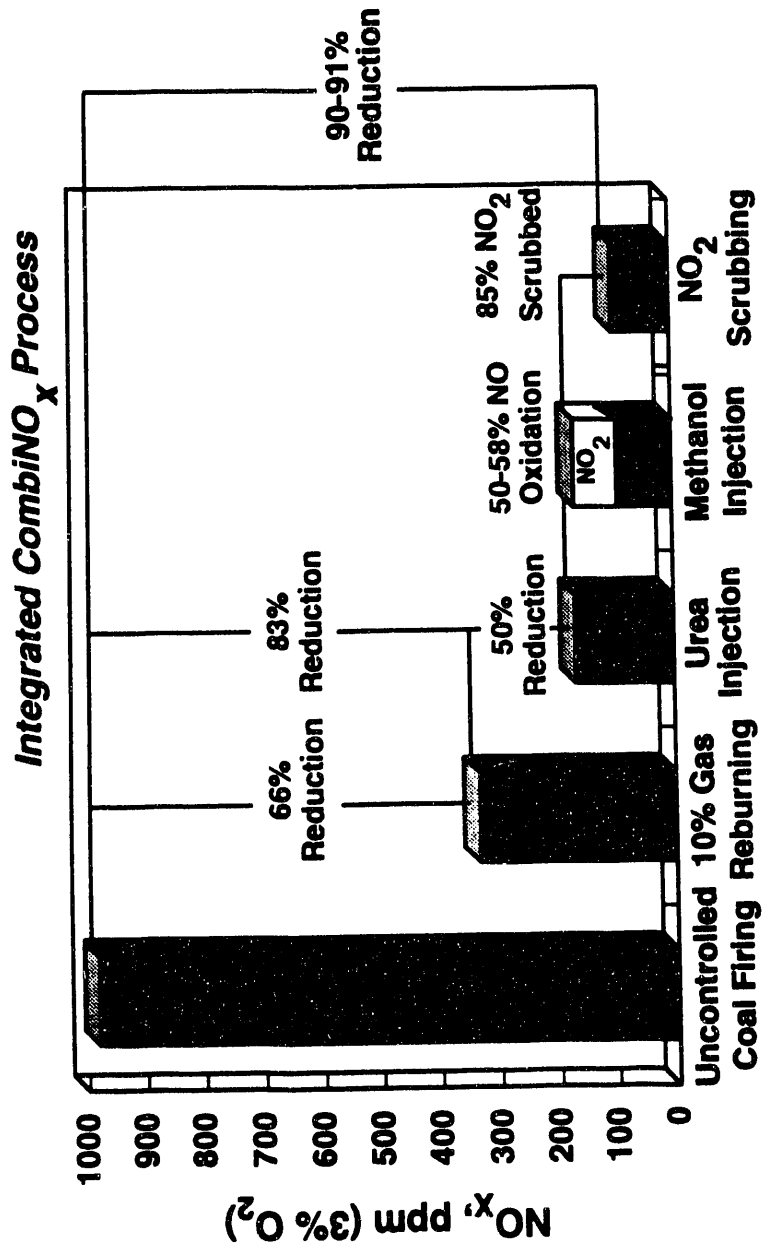


Figure 5-1. NO<sub>x</sub> reduction for integrated Comb<sub>x</sub>NO<sub>x</sub> process at the Reburn Tower.

**END**

---

**DATE  
FILMED**

**5 / 20 / 93**



